

Risk-aware Trading Portfolio Optimization

Marco Bianchetti^{1,2,†}, Gabriele D’Acunto^{*3}, Gianmarco De Francisci Morales⁴,
Yuko Kuroki⁴, Marco Scaringi^{†5}, and Fabio Vitale⁴

¹Financial & Market Risk Management, Intesa Sanpaolo, Milan, Italy

²Department of Statistical Sciences “Paolo Fortunati”, University of Bologna, Italy

³Department of Information Engineering, Electronics and Telecommunications, Sapienza
University, Rome, Italy

⁴CENTAI, Turin, Italy

⁵Risk Trading Quant Department, ING Bank N. V., Milan, Italy

[†]Corresponding author, marco.bianchetti@unibo.it

Abstract

We investigate portfolio optimization in financial markets from a trading and risk management perspective. We term this task Risk-Aware Trading Portfolio Optimization (RATPO), formulate the corresponding optimization problem, and propose an efficient Risk-Aware Trading Swarm (RATS) algorithm to solve it. The key elements of RATPO are a generic initial portfolio \mathcal{P} , a specific set of Unique Eligible Instruments (UEIs), their combination into an Eligible Optimization Strategy (EOS), an objective function, and a set of constraints. RATS searches for an optimal EOS that, added to \mathcal{P} , improves the objective function respecting the constraints.

RATS is a specialized Particle Swarm Optimization method that leverages the parameterization of \mathcal{P} in terms of UEIs, enables parallel computation with a large number of particles, and is fully general with respect to specific choices of the key elements, which can be customized to encode financial knowledge and needs of traders and risk managers.

We showcase two RATPO applications involving a real trading portfolio made of hundreds of different financial instruments, an objective function combining both market risk (VaR) and profit&loss measures, constrains on market sensitivities and UEIs trading costs. In the case of small-sized EOS, RATS successfully identifies the optimal solution and demonstrates robustness with respect to hyper-parameters tuning. In the case of large-sized EOS, RATS markedly improves the portfolio objective value, optimizing risk and capital charge while respecting risk limits and preserving expected profits.

Our work bridges the gap between the implementation of effective trading strategies and compliance with stringent regulatory and economic capital requirements, allowing a better alignment of business and risk management objectives.

*The work of Gabriele D’Acunto was supported by CENTAI Institute, Turin, Italy, and conducted during his affiliation with the Institute.

[†]The present study was conducted while Marco Scaringi was affiliated with Financial & Market Risk Management, Intesa Sanpaolo, Milan, Italy.

Contents

| | | |
|----------|---|-----------|
| 1 | Introduction | 3 |
| 2 | Preliminaries | 6 |
| 3 | Risk-aware trading portfolio optimization | 9 |
| 4 | Risk-aware trading swarm algorithm | 11 |
| 5 | Empirical assessment | 14 |
| 5.1 | Experimental setting | 15 |
| 5.2 | Comparison with the Markowitz-like approach | 18 |
| 5.3 | Small-sized eligible optimization strategy | 20 |
| 5.4 | Large-sized eligible optimization strategy | 22 |
| 6 | Conclusions and perspectives | 24 |
| | References | 25 |
| A | Hyper-parameters | 28 |
| B | Data for UEIs | 28 |
| C | Running time | 31 |
| D | Estimated parameters for Euro Stoxx 50 Index | 32 |

JEL classifications: D8, H51.

MSC Classification: 35A01, 65L10, 65L12, 65L20, 65L70.

Keywords: Portfolio optimization, risk management, trading, particle swarm optimization.

Acknowledgements: the authors contributed equally to this work. The authors acknowledge fruitful discussions with many colleagues from Intesa Sanpaolo Risk Management and Front Office Departments, Francesco Terribile and Pietro Gallo from Politecnico di Milano, who collaborated to the early stage of this work, Luca Lamorte, who joined at later stage, and Laura Li Puma, Arianna Miola, and Luigi Ruggerone from Intesa Sanpaolo Innovation Center for supporting the research team. Marco Scaringi declares that the views and opinions expressed here are his own and do not represent the views of his previous or current employers; they are not responsible for any use that may be made of these contents.

1 Introduction

The financial crisis started in 2007, and the subsequent period of severe market stresses revealed weaknesses in the risk capital framework of the global banking and financial system. Since then, regulators increased pressure towards risk-based capital reserves. The Basel Committee on Banking Supervision (BCBS), the main international body that develops global banking standards, issued the so-called Basel III and Basel IV accords (Basel Committee on Banking Supervision 2011; Basel Committee on Banking Supervision 2017), introducing substantial amendments to the capital treatment of all risk classes (market, liquidity, counterparty, credit and operational risk).¹ The BCBS proposals are transposed into legal frameworks by national and international authorities.²

The trading and risk management practices of financial institutions has developed according to regulatory requests. Nowadays, banks typically put huge efforts into research, development, implementation, and production of several different risk measures, which are the main inputs to compute capital reserves, both for regulatory purposes (regulatory capital and Risk-Weighted Assets—RWA) and internal managerial purposes (economic capital). In particular, market risk measures (e.g., Value at Risk, Stressed Value at Risk, Incremental Risk Charge) are typically computed with daily frequency, both for managerial reporting to trading desks, and to determine quarterly averages for regulatory reporting of capital reserves. Budgets for human and IT resources for risk management purposes have increased accordingly.

Our goal: risk-aware trading portfolio optimization In the “classic” portfolio optimization approach à la Markowitz (Markowitz 1952), the point of view of portfolio managers typically prevails, who focus on *dynamic* forward-looking estimates of return and risk by selecting a portfolio of assets and looking for a strategy to adjust the assets’ weights over a given time horizon $T - t$, where t is the rebalancing date.

In this work, we focus on a different problem, named *risk-aware trading portfolio optimization*, where we take the point of view of the bank’s traders and risk managers, who focus on *statical* portfolio risk measurement and features at a given point in time t , and look for optimal trades at the same time t to reduce capital reserves while preserving portfolio value, consistently with the business objectives. This view, characterizing our approach, represents a stark difference with Markowitz’s framework.

Another distinguishing feature of our approach concerns the full generality with respect to the portfolio composition. More in detail, we consider *large heterogeneous trading portfolios* typical of commercial or investment banks, potentially encompassing millions of financial instruments such as stocks, securities, loans, derivatives, and funds, depending on any underlying *risk factors*, i.e., interest rates, credit, equity, forex, and commodities. These positions can feature any level of *complexity*: linear and non-linear payoffs, plain vanilla and exotic options, multi-asset and hybrid derivatives. They are managed through appropriate pricing models and computational algorithms such as analytical formulas and Monte Carlo simulations. Moreover, trading portfolios are characterized by continuous *turnover*, driven by expiry of old trades, flows of new trades with clients, proprietary investments, speculative or hedging strategies, and generate continuous in/out cash flows related to received/paid coupons, collateral exchange, financing operations, and fees.

¹The BCBS also maintains the “Basel Framework” (https://www.bis.org/basel_framework) which provides a comprehensive and updated compendium of BCBS financial regulations.

²The European Union transposed the after-crisis BCBS proposals into the so-called CRD4/CRR package in 2013 (CRD4 2013; CRR1 2013), the amended CRD5/CRR2 package in 2019 (CRD5 2019; CRR2 2019), and the further amended CRD6/CRR3 package in 2024 (CRD6 2024; CRR3 2024), the latter to enter into force in January 2025 and January 2026, respectively. The European Banking Authority (EBA) maintains the Interactive Single Rulebook (<https://www.eba.europa.eu/single-rulebook>) which provides a comprehensive compendium of EU financial regulations and related Q&As.

Furthermore, in our approach portfolio risks are measured through various *risk measures* that capture all the different risk sources, e.g., market risk, liquidity risk, credit and counterparty risk, and valuation risk.³ These risks are managed within a global Risk Appetite Framework (RAF)⁴, a structured approach used by Banks to define, manage, and align their willingness to assume risks in pursuit of their business objectives. The RAF is based on *risk limits*, which are set, monitored, and reported by a risk management unit independent of business units.

Core components Several crucial components characterize our risk-aware trading portfolio optimization approach. *unique eligible instruments* are the main building blocks used to optimize the portfolio: they uniquely identify liquid market instruments quoted by exchanges, brokers, or market makers, typically used by traders for risk management purposes, i.e., to hedge Delta, Vega, and Gamma risks. Portfolio optimization is encoded through *eligible optimization strategies*, i.e., combinations of unique eligible instruments added to the portfolio to optimize the selected *objective function*, while complying with a set of *constraints* and adhering to a specific *structure* reflecting the prior financial knowledge of the bank’s traders and risk managers. The objective function consists of a combination of portfolio risk measures and features such as profit and loss measures and market transaction costs. Instead, the constraints are associated with risk limits to effectively drive the optimization process. More details and practical examples of these core components are included in the following sections.

Challenges Our risk-aware trading portfolio optimization problem presents numerous challenges. The objective function is typically non-linear and its computation, particularly in the case of risk measures based on historical or Monte Carlo simulation, can require substantial computational resources. The unique eligible instruments are determined by various parameters, which are either intrinsically categorical (e.g., payoff type, currency, underlying asset), or are quoted in market-discrete values (e.g., maturity, strike), though some can be approximated continuously (e.g., notional amounts). Hence, a candidate eligible optimization strategy is represented by a set of values of the relevant parameters.

However, the sheer number of potential combinations of the parameters’ values makes the brute-force approach (i.e., the direct calculation of all possible solutions) unfeasible even for simple portfolios and optimization strategies. Additionally, not every optimization strategy satisfies the optimization constraints, depending on their tightness (the tighter the constraints, the fewer eligible solutions). Finally, the global optimal solution is often hidden among numerous similar local optima due to the inherent complexity of the objective function landscape.

Optimization meta-heuristics From a computational point of view, we must solve a multidimensional, non-linear, constrained optimization problem with integer variables, where the value of the objective function may change abruptly, thus complicating the search for a global minimum. Since simple techniques are insufficient for such complex problems, numerical algorithms based on *optimization meta-heuristics* are typically used. These techniques are recognized as efficient approaches for optimization problems that cannot be exactly solved in a “reasonable” time limit, overcoming incomplete initial information or limited computation capacity, and sampling a portion of the entire set of solutions that is too large to be completely explored. Even though these algorithms do not guarantee to converge to the global optimum in a finite computational time, their application to our optimization problem is beneficial, since also local optima leading to appreciable improvements of the objective function are valuable from a financial point of view.

³Valuation risk is captured by appropriate *valuation risk measures* such as fair value adjustments, required by EU accounting standards (IFRS, <https://www.ifrs.org>), and Additional Valuation Adjustments (AVA) deducted from Common Equity Tier 1 capital, required by EU prudential regulation (CRR3 2024), etc., which ultimately determine the capital structure of the Bank.

⁴RAF guidelines are issued by the Basel Committee of Banking Supervision (Basel Committee on Banking Supervision 2015) and transposed by the EU into CRD/CRR packages.

A complete overview of optimization meta-heuristics is presented by Boussaid, Lepagnot, and Siarry 2013, who distinguish between *single solution based* algorithms, such as Simulated Annealing (Kirkpatrick, Gelatt, and Vecchi 1983), which start with a single initial solution and move along a trajectory in the search space, and *population based* algorithms, which explore the search space using a population of different solutions evolving according to some rules, such as Genetic Algorithms (GA, Holland 1992), and Particle Swarm Optimization (PSO, Kennedy and Eberhart 1995).

Related literature The classic portfolio optimization problem following Markowitz 1952 is widely discussed in the literature, also using optimization meta-heuristics (Dallagnol, Berg, and Mous 2009; Soleimani, Golmakani, and Salimi 2009) and even quantum computers (Rosenberg et al. 2016; Venturelli and Kondratyev 2019). Conversely, to the best of our knowledge, the risk-aware trading portfolio optimization problem introduced above represents an understudied topic. Our work was initially motivated by Kondratyev and Giorgidze 2017, who use GA and PSO meta-heuristics to search optimal delta hedging strategies in the context of Margin Valuation Adjustment optimization.⁵ This seminal work is limited to a specific and very simple setting: a toy portfolio of USDCNY Non Deliverable FX Forwards (NDF, i.e., linear instruments on a single exchange rate) exchanged between two out of five counterparties, one single optimization instrument (the USDCNY NDF itself), and no optimization constraints beyond trading cost. An apparent application to collateral optimization with multiple Central Counterparties is found in Erekhinsky 2017.

The idea of portfolio optimization based on market risk measures is obviously not new. For example, Rockafellar and Uryasev 2000 and Larsen, Mausser, and Uryasev 2002 minimize Conditional Value at Risk (a.k.a. Expected Shortfall) using analytical approaches and linear programming techniques. Gaivoronski and G. Pflug 2005 determine an optimal Value at Risk portfolio with a given expected return. Gilli, Kellezi, and Hysi 2006 determine optimal quantities of n assets which minimize different risk functions for a given return target under constraints on the assets' sizes. J. Faias and Santa-Clara 2011, J. A. Faias and Santa-Clara 2017 and Dao 2014 consider simplified European options' portfolios.

Also the idea of portfolio optimization based on meta-heuristics is largely explored in the literature. T.-J. Chang, Yang, and K.-J. Chang 2009 solve portfolio optimization problems by employing GA and risk measures based on Markowitz's mean-variance, semi-variance, mean absolute deviation, and variance with skewness. Deng, Lin, and C.-C. Lo 2012 introduce an improved PSO to solve the Cardinality Constraints Markowitz Portfolio Optimization problem. Das et al. 2023 compare PSO, GA, Dynamic Programming, and Differential Evolutionary Algorithm algorithms for portfolio optimization in the NIFTY 50 market using Sharpe Ratio and expected return. Jun and Johar 2023 use PSO to maximize the Sharpe Ratio of portfolios of Exchange-Traded Funds, demonstrating its effectiveness in achieving higher risk-adjusted returns compared to traditional methods. Erwin and Engelbrecht 2023b develop a Multi-Guide Set-Based Particle Swarm Optimization for multi-objective portfolio optimization, and test it against established algorithms.

Excellent reviews by Fabozzi, Huang, and Zhou 2010, Ertenlice and Kalayci 2018, Erwin and Engelbrecht 2023a, Loke et al. 2023 and Gunjan and Bhattacharyya 2023 are available. Erwin and Engelbrecht 2023a review 140 studies using evolutionary and swarm intelligence algorithms for portfolio optimization, finding that meta-heuristic approaches as more computationally efficient.

Our contributions With the partial exception of Kondratyev and Giorgidze 2017, none of the cited works addresses the challenges of the risk-based trading portfolio optimization problem investigated in this paper. Specifically, our contributions are outlined below.

⁵Margin Valuation Adjustment is a valuation adjustment which takes into account the cost of financing initial margin collateralization of OTC derivatives, see e.g. Gregory 2020; Green 2015.

- We introduce and formalize the risk-aware trading portfolio optimization problem, taking the point of view of the bank’s traders and risk managers. Toward our goal, we introduce and consequently leverage the key concepts of the unique eligible instruments and eligible optimization strategies, also including options to allow Delta, Vega, and Gamma optimization.
- We propose a modified PSO algorithm, called *Risk-Aware Trading Swarm* (RATS), incorporating a specialized parameterization built around the concepts of the unique eligible instruments and eligible optimization strategy. RATS is a versatile framework that leverages the parallelizable nature of the optimization problem with respect to the particle dimension and can be adapted to different trading portfolios, objective functions, and constraints. Additionally, its parameterization enables users to incorporate their financial insights and business views by directly shaping the structure of the eligible optimization strategies.
- We showcase two applications on a real trading portfolio typical of large banks, made of hundreds of financial instruments of different kinds, using real market data and tradable optimization instruments. In both cases, we seek an eligible optimization strategy that, when combined with the initial portfolio, optimizes a fractional, non-convex objective function over a non-convex set of eligible optimization strategies defined by the constraints. Inspired by the practical needs of traders and risk managers, the objective function accounts for the Value at Risk measure, expected P&L, and trading costs. In addition, the set of constraints includes sensitivity limits; while the size of the eligible optimization strategy, its diversification, and the maximum nominal amount are handled directly via the proposed parameterization. In the first application, focused on a small-sized optimization strategy, RATS successfully identifies an optimal solution within the optimal solution set and demonstrates robustness to hyper-parameters tuning across all tested scenarios. In the second application, involving a large-sized optimization strategy, RATS markedly improves the cost-adjusted expected P&L and risk measures of the initial portfolio in every setting.

At a high level, our work overcomes our inspiring paper by Kondratyev and Giorgidze 2017 and bridges the gap between complying with stringent regulatory requirements and implementing effective trading strategies that align with the objectives of both business units and risk management.

Roadmap This paper is organized as follows. Section 2 provides the fundamental concepts underlying the risk-aware trading portfolio problem. Then, Section 3 formalizes the risk-aware trading portfolio optimization problem. Next, Section 4 describes the proposed method, i.e., RATS. Section 5 provides the results of our empirical assessment. In detail, Section 5.1 specifies the setting and the building blocks of the risk-aware trading portfolio optimization problem. Section 5.2 compares our approach to Markowitz-like approaches, highlighting their limitations and key differences. Subsequently, Section 5.3 explores the small-sized application setting, and Section 5.4 addresses the large-sized one. Finally Section 6 draws the conclusions and outlines future research directions.

2 Preliminaries

This section provides the basic notation and key concepts that underlie the risk-aware trading portfolio problem. We start the discussion at the individual financial instrument level and then move to the portfolio level.

Notation We denote by $[n]$ the set $\{1, 2, \dots, n\}$ with $n \in \mathbb{N}$. Scalars are lowercase letters, a , vectors are lowercase bold, \mathbf{a} , matrices are uppercase bold, \mathbf{A} , sets are uppercase calligraphic, \mathcal{A} , elements of a set are uppercase, A . Given a , we denote $\max(a, 0)$ by $[a]_+$. The multiset union operator is \uplus . The element-wise (Hadamard) product is denoted by \circ . We use subscripts for

indices, while superscripts are used for everything else. Given an n -dimensional vector \mathbf{a} and a permutation \prec such that $\mathbf{a}^\prec = [a_1^\prec, \dots, a_n^\prec]$ is increasing, we denote by $\mathcal{S}(\cdot)$ the sort operator such that $\mathbf{a}^\prec = \mathcal{S}(\mathbf{a})$. The discrete uniform distribution is $U\{a, b\}$, whereas the continuous one is $U(a, b)$. We work in a *static* setting, that is, a fixed point in time t . Hence, throughout the paper, we omit any reference to time without any ambiguity, also to ease the notation.

Unique instruments We consider financial instruments of any type, such as fundamental assets (e.g., stocks), derivatives (e.g., swaps, options), securities (e.g., government and corporate bonds), and loans (e.g., mortgages). We identify a financial instrument having a unitary nominal amount with a set of m (categorical) parameters, namely $\{\phi_1, \dots, \phi_m\}$. The parameters ϕ_i can vary in their corresponding domains \mathcal{D}^{ϕ_i} . We term the sequence given by concatenating the values of the latter parameters *unique instrument* (UI). For instance, consider a vanilla option. A possible parameterization is given by four parameters, i.e., the ticker of the underlying, the payoff type, the strike, and the time-to-maturity. In this case, a UI is a sequence obtained by concatenating the four values of the previous parameters, each belonging to the associated domain. Additional parameters can be considered according to the application need (e.g., currency, dividends, counterparty).

Risk factors and risk scenarios The UI is associated with a set of random variables $\mathcal{R} = \{R_1, \dots, R_n\}$, called *risk factors*, which fully determine its price. For instance, in the case of an option, key risk factors are the price of the underlying S , the implied volatility σ , the interest rate R , and the dividend rate D . Each risk factor can be associated with a risk distribution, quantifying the likelihood of different values in the risk factor. Hence, estimating the risk distribution enables the simulation of risk scenarios for the risk factor. We denote the dataset of risk scenarios by \mathcal{F} .

Unique instruments features Features can characterize unique instruments, and we generally refer to them as φ^G . They can be either observed on the market, thus part of the market data \mathcal{M} , or computed by using risk factors \mathcal{R} and risk scenarios \mathcal{F} . Below we provide those relevant to our empirical assessment in Section 5.

Value. Consider a UI, namely G . We indicate its *value* by v^G . The value can be either *marked to market*, in which case the value is quoted on the market, or *marked to model*, when the value is computed using a specific pricing model involving the relevant risk factors. Pricing models can be chosen according to the institution's internal pricing policy. Additionally, they may be calibrated to their reference plain vanilla instruments, and may be based on different numerical approaches (e.g., analytical formulas or Monte Carlo simulations).

Profit and loss. The proposed framework is based on historical scenarios of risk factors \mathcal{F} and the corresponding *profit and loss* (P&L) distribution. These scenarios simulate past market variations at a fixed point in time t to assess changes in the UI value. Consider s simulated scenarios. We obtain s historical P&L r_i^G , with $i \in [s]$, as follows. Denote by v_0^G and v_i^G the value of the UI at t and at the i -th simulated scenario, respectively. Hence, we have

$$r_i^G = v_i^G - v_0^G, \quad i \in [s]. \quad (1)$$

We arrange the previous historical P&L in the vector $\mathbf{r}^G = [r_1^G, \dots, r_s^G]^\top$.

Greeks. UIs can be characterized by the sensitivity of their value v^G to changes in the underlying risk factors \mathcal{R} . These sensitivities are known as *Greeks*. We introduce below the most important Greeks typically used for risk management and trading purposes. *Delta* is the sensitivity of v^G with respect to changes in the underlying price S^G ,

$$\Delta^G = \frac{\partial v^G}{\partial S^G}. \quad (2)$$

Vega is the sensitivity of v^G with respect to changes in the implied volatility of the underlying asset σ^G ,

$$\mathcal{V}^G = \frac{\partial v^G}{\partial \sigma^G}. \quad (3)$$

Gamma is the sensitivity of Delta with respect to changes in the underlying price S^G ,

$$\Gamma^G = \frac{\partial^2 v^G}{\partial S^{G^2}}. \quad (4)$$

Trading cost. Trading financial instruments incurs trading costs. It is market practice to measure such costs in terms of sensitivity, i.e., Delta for linear instruments and additionally Vega for options. Given a UI, namely G , we denote such contributions deriving from the buying of a unitary notional amount of G by c^{Δ^G} and $c^{\mathcal{V}^G} \in \mathbb{R}^+$, respectively. Hence, the cost for buying a unitary notional amount of G is

$$c^G = c^{\Delta^G} + c^{\mathcal{V}^G}. \quad (5)$$

The computation of c^{Δ^G} and $c^{\mathcal{V}^G}$ is specific to the nature of G . Henceforth, we provide the cases of stocks, futures on equity indexes, and European call and put options, which are instrumental for the empirical assessment in Section 5.

Denote by (i) δ the market bid/ask spread for the underlying corresponding to G , (ii) δ^q the market bid/ask spread for futures, and (iii) δ^K the market bid/ask spread for the European options with strike K (expressed as Delta-percentage). The cost contributions for the corresponding UIs are

$$c^{\Delta^G} = \begin{cases} \frac{1}{2} \Delta^G \delta & \text{if } G \text{ is either a stock, or a call, or a put,} \\ \frac{1}{2} \delta^q & \text{if } G \text{ is a futures;} \end{cases} \quad (6)$$

and

$$c^{\mathcal{V}^G} = \begin{cases} \frac{1}{2} \mathcal{V}^G \delta^K & \text{if } G \text{ is either a call or a put,} \\ 0 & \text{otherwise.} \end{cases} \quad (7)$$

Portfolio parameterization A portfolio is canonically viewed as a collection of financial instruments with nominal amounts different from zero. The value of a financial instrument may be specified in terms of a unitary value in a given currency times the notional amount. In our setting, the unitary value is the value v^G of the corresponding UI. Accordingly, we represent the portfolio as a pair $\langle \mathcal{G}, \mathbf{g} \rangle$, where $\mathcal{G} = \{G_1, \dots, G_n\}$ is the set of UIs in the portfolio, and $\mathbf{g} = [g_1, \dots, g_n]^\top$ is the integer vector of their corresponding notional amounts, representing long and short positions. Such portfolio parameterization is particularly convenient during optimization. First, it enables the search on UIs and nominal amounts to be separated. Second, it allows the portfolio features and risk measures to be expressed in terms of those of the constituting UIs. Accordingly, we can compute relevant features and risk measures at the UI level during the initialization phase. Then, instead of recomputing from scratch the portfolio features and risk measures by means of pricing functions at each iteration, we exploit the stored values during the optimization process thus reducing the computational burden (see Section 4).

Portfolio features As in the case of the UI, we can associate features with a financial portfolio. By exploiting the parameterization $\langle \mathcal{G}, \mathbf{g} \rangle$, the portfolio feature $\varphi(\mathcal{G}, \mathbf{g})$ can be written as a linear combination of the UIs' feature φ^{G_j} , where the coefficients $a(g_j)$ depend on the notional amount associated with each UI. Mathematically,

$$\varphi(\mathcal{G}, \mathbf{g}) = \sum_j^n a(g_j) \varphi^{G_j}. \quad (8)$$

Starting from Equations (1) to (5), exploiting Equation (8), the portfolio features relevant to our empirical assessment read as

$$\begin{aligned}
v^{\mathcal{G}} &= \sum_j^n g_j v^{G_j}, & (\text{Value}) \\
r_i^{\mathcal{G}} &= \sum_j^n g_j r_i^{G_j}, & (\text{P\&L for the } i\text{-th risk scenario, } i \in [s]) \\
\Delta^{\mathcal{G}} &= \sum_j^n g_j \Delta^{G_j}, & (\text{Delta sensitivity}) \\
\mathcal{V}^{\mathcal{G}} &= \sum_j^n g_j \mathcal{V}^{G_j}, & (\text{Vega sensitivity}) \\
\Gamma^{\mathcal{G}} &= \sum_j^n g_j \Gamma^{G_j}, & (\text{Gamma sensitivity}) \\
c^{\mathcal{G}} &= \sum_j^n c^{G_j} |g_j|. & (\text{Trading cost})
\end{aligned} \tag{9}$$

As per the UI, we arrange the historical P&L of the portfolio in a vector, namely $\mathbf{r}^{\mathcal{G}} = [r_1^{\mathcal{G}}, \dots, r_s^{\mathcal{G}}]$. Additionally, the trading cost involves the absolute notional amount since the trading fee is paid for both long and short trades.

Risk measures Starting from the vector of portfolio P&L, we estimate the portfolio *risk measures*, generally denoted by $\rho(\mathcal{G}, \mathbf{g})$. Below we report those relevant to our application in Section 5. We remark that our framework is general, and is not limited to using such risk measures.

First, we have the *sample profit and loss*

$$\overline{\text{P\&L}}^{\mathcal{G}} = \frac{1}{s} \sum_i^s r_i^{\mathcal{G}}, \tag{10}$$

namely the empirical mean of the vector of portfolio P&L.

Second, the *sample Value at Risk at the β percentile*, namely $\beta\text{-VaR}^{\mathcal{G}}$, obtained using decreasing scenarios weight. Consider $\lambda \in (0, 1)$ the decay factor used to give more weight to the most recent scenarios, and define $\alpha = 1 - \beta(1 - \lambda^s)$. Then, setting $i^* = \lceil \ln \alpha / \ln \lambda \rceil$, we have

$$\beta\text{-VaR}^{\mathcal{G}} = [\mathcal{S}(\mathbf{r}^{\mathcal{G}})]_{i^*}, \tag{11}$$

viz., $\beta\text{-VaR}^{\mathcal{G}}$ is the i^* -th entry of the vector of sorted portfolio P&L.

3 Risk-aware trading portfolio optimization

At a high level our goal can be stated as follows. Consider an initial portfolio $\langle \mathcal{P}, \mathbf{p} \rangle$ at time t and an objective function f , which will be discussed below. Additionally, consider a set of risk- and trading-based constraints associated with portfolio features and risk measures. We want to find the portfolio $\langle \mathcal{T}, \mathbf{t} \rangle$ optimizing f , which is obtained by adding to $\langle \mathcal{P}, \mathbf{p} \rangle$ a suitable *eligible optimization strategy* (EOS), denoted by $\langle \mathcal{H}, \mathbf{h} \rangle$, complying with the specified constraints. Mathematically,

$$\langle \mathcal{T}, \mathbf{t} \rangle := \left\langle \mathcal{P} \uplus \mathcal{H}, \left[\mathbf{p}^\top, \mathbf{h}^\top \right]^\top \right\rangle. \tag{12}$$

We call this task *risk-aware trading portfolio optimization* (RATPO). In the sequel, we formulate the general RATPO problem.

Looking at RATPO, the first key ingredient is the initial portfolio $\langle \mathcal{P}, \mathbf{p} \rangle$. In our work, \mathcal{P} may include any UI, as assumed throughout Section 2. The parameterization of such UIs is static and does not depend on the specification of RATPO. Accordingly, we call \mathcal{P} the set of *unique static instruments*. Analogously, the vector of notional amounts $\mathbf{p} \in \mathbb{Z}^{|\mathcal{P}|}$ is fixed during the optimization process.

The second key ingredient is the objective function f . Consider (i) a set of p portfolio risk measures, $\rho_i(\mathcal{T}, \mathbf{t})$, $i \in [p]$; and (ii) a set of q portfolio features $\varphi_j(\mathcal{T}, \mathbf{t})$, $j \in [q]$. The family of objective functions considered in RATPO is a general combination of (possibly nonconvex) risk measures and portfolio features. Specifically,

$$f(\mathcal{T}, \mathbf{t}) \stackrel{(a)}{=} f(\mathcal{H}, \mathbf{h}; \mathcal{P}, \mathbf{p}) := f(\rho_1, \dots, \rho_p, \varphi_1, \dots, \varphi_q); \quad (13)$$

where in (a) we recognize that $\langle \mathcal{P}, \mathbf{p} \rangle$ is fixed during the optimization. Additionally, in Equation (13) we omit the arguments for risk measures and the portfolio features to enhance readability. The specific risk measures, portfolio features, and functional form of f can be chosen according to the application's need, as demonstrated in the empirical assessment in Section 5.

The third key ingredient is a set of z inequality and equality constraints, $\psi_i(\mathcal{H}, \mathbf{h}; \mathcal{P}, \mathbf{p})$, $i \in [z]$. Similarly to the objective function, each constraint can be a combination of (possibly nonconvex) risk measures and portfolio features, depending on the application need. The constraints entail the set of *feasible* EOS, denoted by \mathcal{E} , which can be nonconvex.

Next, the fourth key ingredient is the total portfolio $\langle \mathcal{T}, \mathbf{t} \rangle$. Starting from Equation (12), the considered *universe* of UIs in RATPO, namely \mathcal{U} such that $\mathcal{T} \subseteq \mathcal{U}$, consists of the multiset union of two distinct sets. The first, \mathcal{P} , is the set of UIs in the initial portfolio. The second, $\mathcal{U}^{\mathcal{H}}$ such that $\mathcal{H} \subseteq \mathcal{U}^{\mathcal{H}}$, is the set of all possible UIs constituting the EOS $\langle \mathcal{H}, \mathbf{h} \rangle \in \mathcal{E}$. The set $\mathcal{U}^{\mathcal{H}}$ depends on the specification of RATPO since it is entailed by the Cartesian product of the domains \mathcal{D}^{ϕ_i} associated with the parameters ϕ_i specifying each UI H_j that can constitute \mathcal{H} , where $j \in [|\mathcal{U}^{\mathcal{H}}|]$. We term the H_j *unique eligible instrument* (UEI), and $\mathcal{U}^{\mathcal{H}}$ the set of UEIs. Note that some UIs in \mathcal{P} can potentially be in $\mathcal{U}^{\mathcal{H}}$, depending on the application's need. This is the reason why we use the multiset union. Now, we can pose the formal definitions for the UEI and for the EOS.

Definition 1 (Unique eligible instrument, UEI). *A unique eligible instrument $H_j \in \mathcal{U}^{\mathcal{H}}$ refers to a financial instrument tradable on the market at the optimization time t . It is represented as the sequence resulting from the concatenation of a combination in the Cartesian product $\mathcal{D}^{\phi_1} \times \dots \times \mathcal{D}^{\phi_m}$, where ϕ_1, \dots, ϕ_m are the parameters determining the UEI, and $\mathcal{D}^{\phi_1}, \dots, \mathcal{D}^{\phi_m}$ the corresponding domains.*

Definition 2 (Eligible optimization strategy, EOS). *An eligible optimization strategy $\langle \mathcal{H}, \mathbf{h} \rangle$ is a tradable financial strategy at time t , complying with a set of specified constraints. It is a set $\mathcal{H} \subseteq \mathcal{U}^{\mathcal{H}}$ of UEIs, weighted by the corresponding notional amounts $h_j \in \mathbf{h}$, such that $\langle \mathcal{H}, \mathbf{h} \rangle \in \mathcal{E}$.*

At this point, we are ready to formally state the general RATPO problem.

Problem 1 (Risk-aware trading portfolio optimization, RATPO). *Given an initial portfolio $\langle \mathcal{P}, \mathbf{p} \rangle$, the total portfolio that optimizes the objective function f is given by $\langle \mathcal{T}^*, \mathbf{t}^* \rangle := \left\langle \mathcal{P} \uplus \mathcal{H}^*, \left[\mathbf{p}^\top, \mathbf{h}^{*\top} \right]^\top \right\rangle$, where*

$$\langle \mathcal{H}^*, \mathbf{h}^* \rangle = \arg \min_{\langle \mathcal{H}, \mathbf{h} \rangle \in \mathcal{E}} f(\mathcal{H}, \mathbf{h}; \mathcal{P}, \mathbf{p}). \quad (\text{P1})$$

The optimization variable in (P1), i.e., the EOS $\langle \mathcal{H}, \mathbf{h} \rangle$, can be mapped into an integer vector as further discussed in Section 4. Thus, Problem (P1) can be viewed as an integer optimization problem with possibly nonconvex objective function and constraint set. We emphasize that nonconvexity can easily originate from the risk measures and portfolio features considered by risk managers and traders in their daily activities. Hence, the difficulty in solving (P1) boils down to the mathematical properties of the objective function in Equation (13) and of the feasible solution set \mathcal{E} . Establishing a general method that guarantees global convergence for the general RATPO problem is not feasible, and each specification of (P1) should be analyzed separately. The next section exposes a general-purpose algorithm based on particle swarm optimization. This method empirically proves to be effective and efficient in solving an instance of the RATPO problem involving the main risk measures and portfolio features used in daily risk management and trading activities (see Section 5).

4 Risk-aware trading swarm algorithm

Meta-heuristics represent general-purpose approaches for solving optimization problems. Among their features, they do not make restrictive assumptions on the mathematical properties of the objective function and constraints. This approach allows risk managers and traders to specify arbitrarily complex objective functions of the form in Equation (13) arising from the need to satisfy trading, risk management, and regulatory objectives. In addition, this aspect allows specifying complex constraints set, and thus guiding the optimizer’s search toward solutions to problem (P1) having precise financial meaning. In addition, they do not leverage the gradient during the optimization. Therefore, they are amenable to handling optimization variables of different natures. Finally, they efficiently explore the solution space by balancing the exploration-exploitation trade-off (see. Erwin and Engelbrecht 2023a).

The compromise for this flexibility is the lack of convergence guarantees to a global optimum within a finite time. These algorithms may become trapped in local optima, making it challenging to assess their proximity to the global optimum. Nonetheless, for risk managers and traders—who typically possess deep domain knowledge that can inform the optimization problem through constraints—a consistent reduction in the objective function remains valuable.

In our work, we build upon *particle swarm optimization* (PSO), originally introduced by Kennedy and Eberhart 1995. PSO is inspired by the flocking behavior of birds and fishes, and represents one of the most popular meta-heuristics based on the *swarm intelligence paradigm* by Kennedy 2006. In PSO, each particle in the swarm explores positions, i.e., candidate solutions of the optimization problem, in an n -dimensional space. Specifically, denoting by n^p the number of particles, the particle is described by the position and velocity vectors, \mathbf{x}_i and \mathbf{v}_i , $i \in [n^p]$, respectively. The algorithm proceeds by iteratively updating the particles’ position and velocity vectors. We denote by \mathbf{y}_i^k and \mathbf{z}^k respectively (i) the best position visited by the i -th particle at iteration k , and (ii) the best global position visited by the swarm at iteration k , respectively. Given (i) the *inertia weight* $w \in \mathbb{R}^+$, (ii) the *personal* and *social coefficients* c^{pers} and c^{soc} in \mathbb{R}^+ respectively, and (iii) the vectors \mathbf{r}_1 and \mathbf{r}_2 drawn from $U(0, 1)$, the particle update recursion is

$$\begin{cases} \mathbf{v}_i^{k+1} &= w\mathbf{v}_i^k + \underbrace{c^{\text{pers}}\mathbf{r}_1^{k+1} \circ (\mathbf{y}_i^k - \mathbf{x}_i^k)}_{\text{personal component}} + \underbrace{c^{\text{soc}}\mathbf{r}_2^{k+1} \circ (\mathbf{z}^k - \mathbf{x}_i^k)}_{\text{social component}}, \\ \mathbf{x}_i^{k+1} &= \mathbf{x}_i^k + \mathbf{v}_i^{k+1}. \end{cases} \quad (\text{R1})$$

By building on the key concepts of UEI and EOS, we develop a special version of PSO that leverages the parameterization $\langle \mathcal{H}, \mathbf{h} \rangle$ and enables parallel computation over the particles to efficiently solve the RATPO problem (P1). Our method, termed *risk-aware trading swarm* (RATS), is described below.

Initialization. As a first step, RATS runs an initialization phase. Consider that the cardinality of $\mathcal{U}^{\mathcal{H}}$ is n , and that the names of the UEIs are sorted in lexicographic order. Since each $H_j \in \mathcal{U}^{\mathcal{H}}$

corresponds to a unique combination of the representing parameters' values, we can simply identify the H_j with its index $j \in [n]$ ⁶. Hence, the particle position can be represented as a $2m$ -dimensional integer vector

$$\mathbf{x} := \left[\underbrace{x_1, \dots, x_m}_{\text{UEI indices}}, \underbrace{x_{m+1}, \dots, x_{2m}}_{\text{notional amounts}} \right]^\top, \quad \text{with } m \leq n. \quad (14)$$

The particle position in Equation (14) entails an optimization strategy $\langle \mathcal{H}, \mathbf{h} \rangle$. If $\langle \mathcal{H}, \mathbf{h} \rangle \in \mathcal{E}$, meaning the optimization strategy is *eligible*, the particle position is called *feasible*. Conversely, if $\langle \mathcal{H}, \mathbf{h} \rangle \notin \mathcal{E}$, the particle position is called *unfeasible*. Furthermore, the number of distinct UEIs represented in \mathbf{x} , i.e., $|\mathcal{H}|$, is at most m . This is because, in principle, the first m entries of \mathbf{x} may include repeated indices. Consequently, RATS enables users to easily set an upper bound of m on the number of financial instruments that can be selected, a helpful feature from an application viewpoint.

RATS initializes the entries x_j , $j \in [m]$, by sampling from $U\{b_j, u_j\}$, where b_j and $u_j \in \mathbb{N}$, such that $1 \leq b_j < u_j \leq n$. Hence, users can easily specify the relevant UEIs for each entry x_j through b_j and u_j . Next, RATS initializes the entries x_{j+m} , $j \in [m]$, by sampling from $U\{\ell_j, t_j\}$, where ℓ_j and t_j are minimum and maximum notional amounts, respectively. Thus, ℓ_j and t_j act on the UEIs corresponding to the indices from b_j to u_j within $\mathcal{U}^{\mathcal{H}}$. As far as the velocity vector is concerned, RATS initializes its entries by sampling from $U(v^{\min}, v^{\max})$, where v^{\min} and v^{\max} in \mathbb{R} are two hyper-parameters corresponding to the minimum and maximum velocity.

Additionally, starting from the input datasets of risk factors \mathcal{R} , market data \mathcal{M} , and risk scenarios \mathcal{F} , RATS precomputes the p features of the UEIs relevant to the optimization problem, namely $\varphi_q^{H_j}$ with $q \in [p]$ and $j \in [n]$. This is possible since the features of the UEIs do not change during the optimization process. This way, RATS lowers the computational burden of the optimization process. Indeed, at each iteration k , to assess the goodness and feasibility of the particles' positions \mathbf{x}_i^k , $i \in [n^p]$, we need to compute the features of the optimization strategy entailed by \mathbf{x}_i^k since they are necessary for the evaluation of Equation (13) and of the constraints $\psi_\ell(\mathcal{H}, \mathbf{h}; \mathcal{P}, \mathbf{p})$, $\ell \in [z]$ (cf. Section 2). In general, assessing a feature of an optimization strategy involves evaluating a (nonlinear) function, which can be computationally expensive. On the contrary, RATS efficiently exploits the optimization strategy parameterization which allows us to use Equation (8). Hence, at each iteration and for each particle, the computational cost of the optimization strategy feature evaluation is linear, as it requires $2m - 1$ operations.

Next, RATS evaluates the *fitness* of the initial positions of the particles to set \mathbf{y}_i and \mathbf{z} . Starting from Equation (13), we define the fitness function as

$$\bar{f}(\mathcal{H}, \mathbf{h}; \mathcal{P}, \mathbf{p}) := f(\mathcal{H}, \mathbf{h}; \mathcal{P}, \mathbf{p}) + \sum_{\ell}^z \lambda_{\ell} [\psi_{\ell}(\mathcal{H}, \mathbf{h}; \mathcal{P}, \mathbf{p})]_+. \quad (15)$$

The second term in Equation (15) represents the weighted sum of the violations of the inequality and equality constraints, where $\lambda_j \in \mathbb{R}^+$ are penalty hyper-parameters. If the position is feasible, the value of the fitness function is equal to that of the objective function. Conversely, it is penalized by the weighted sum of constraints' violations. Henceforth, we refer to the fitness function evaluated at the optimization strategy entailed by a particle position \mathbf{x} as $\bar{f}|_{\mathbf{x}}$.

Recursion. After the initialization phase, RATS runs the recursion in (R1) to update the position and the velocity of the particle. In our setting, the particle position \mathbf{x}_i^k takes on values in \mathbb{Z}^{2m} , whereas the velocity vector $\mathbf{v}_i^{k+1} \in \mathbb{R}^{2m}$. Hence, after the second update in (R1), we apply rounding to ensure that \mathbf{x}_i^{k+1} is a vector of integers and its entries are within the specified ranges

⁶The same mapping can be applied to the notional amounts to handle the case in which the notional amount domain is undersampled, that is, the range of the corresponding integers is discretized. We use such a mapping in our empirical assessment in Section 5.

determined by $\{b_j, u_j, \ell_j, t_j\}$, $j \in [m]$. At this point, RATS evaluates $\bar{f}|_{\mathbf{x}_i^{k+1}}$, and accordingly determines \mathbf{y}_i^{k+1} . RATS runs the above steps in parallel over the particles, thus reducing the computational time, and allowing the user to choose larger values of n^p for better exploration. Next, RATS updates the global best position if it finds a new position that improves the fitness function evaluated at the global best position more than τ^f , where $\tau^f \in \mathbb{R}^+$ is a small significance threshold. Specifically, the condition reads as

$$\bar{f}|_{\mathbf{z}^k} - \min_{i \in [n^p]} \bar{f}|_{\mathbf{y}_i^{k+1}} > \tau^f. \quad (16)$$

In case Equation (16) is not satisfied, RATS increases a counter $k^{\text{stall}} \in \mathbb{N}$ which keeps track of the number of stall iterations. Finally, following Shi and Eberhart 1998, we dynamically adjust the inertia weight, according to a linearly decaying rule. Given minimum and maximum values, w^{\min} and w^{\max} , respectively; and setting $w^1 = w^{\max}$, the rule reads as

$$w^{k+1} = w^{\max} - \frac{k}{k^{\max}} (w^{\max} - w^{\min}), \quad (17)$$

where k^{\max} is the maximum number of iterations.

Stopping criteria. RATS exits the recursion either (i) if the maximum number of iterations k^{\max} is reached, or (ii) if the global best position is not updated for a specified number of consecutive stall iterations $k^{\text{stall}} \geq k^{\max \text{stall}}$, or (iii) if the fraction χ of particles exhibiting a personal best position equal to the global best one exceeds a concentration threshold $\tau^p \in (0, 1)$.

Algorithm 1 summarizes the overall procedure. We emphasize that RATS can be easily equipped by the user with different existing variants of PSO.

Algorithm 1: Risk-aware trading swarm (RATS)

Input: risk factors \mathcal{R} , market data \mathcal{M} , risk scenarios \mathcal{F} , initial portfolio $\langle \mathcal{P}, \mathbf{p} \rangle$, unique eligible instruments $\{H_j\}$ with $j \in [n]$, number of particles n^p , minimum/maximum UEI indices/notional amounts $\{b_j, u_j, \ell_j, t_j\}$ with $j \in [m]$, minimum velocity v^{\min} , maximum velocity v^{\max} , minimum inertia weight w^{\min} , maximum inertia weight w^{\max} , small significance threshold τ^f , concentration threshold τ^p , maximum number of iterations k^{\max} , number of consecutive stall iterations $k^{\max \text{stall}}$

Output: \mathbf{z}

```
1  $w \leftarrow w^{\max}$ 
2  $k^{\text{stall}} \leftarrow 0$ 
3 for  $j \leftarrow 1$  to  $n$  do
4   for  $q \leftarrow 1$  to  $p$  do
5      $\varphi_q^{H_j} \leftarrow$  Compute it by using  $\mathcal{R}, \mathcal{M}, \mathcal{F}$ 
6 for  $i \leftarrow 1$  to  $n^p$  do
7    $\mathbf{x}_i^0 \leftarrow$  Sample the first  $m$  entries from  $U\{b_j, u_j\}$ , the rest from  $U\{\ell_j, t_j\}$ , with  $j \in [m]$ 
8    $\mathbf{v}_i^0 \leftarrow$  Sample the entries from  $U(v^{\min}, v^{\max})$ 
9    $\mathbf{y}_i^0 \leftarrow \mathbf{x}_i^0$ 
10   $\bar{f}|_{\mathbf{x}_i^0} \leftarrow$  Apply Equation (15)
11   $\bar{f}|_{\mathbf{y}_i^0} \leftarrow \bar{f}|_{\mathbf{x}_i^0}$ 
12  $\mathbf{z}^0 \leftarrow \arg \min_{\mathbf{y}_i^0} \bar{f}|_{\mathbf{y}_i^0}$ 
13  $\bar{f}|_{\mathbf{z}^0} \leftarrow$  Apply Equation (15)
14 while  $k < k^{\max}$  and  $k^{\text{stall}} < k^{\max \text{stall}}$  and  $\chi < \tau^p$  do
15    $\mathbf{z}^k \leftarrow \mathbf{z}^{k-1}$ 
16    $\mathbf{r}_1, \mathbf{r}_2 \leftarrow$  Sample the entries from  $U(0, 1)$ 
17   do in parallel
18      $\mathbf{y}_i^k \leftarrow \mathbf{y}_i^{k-1}$ 
19      $\mathbf{v}_i^k, \mathbf{x}_i^k \leftarrow$  Apply (R1)
20      $\bar{f}|_{\mathbf{x}_i^k} \leftarrow$  Apply Equation (15)
21     if  $\bar{f}|_{\mathbf{x}_i^k} < \bar{f}|_{\mathbf{y}_i^k}$  then
22        $\mathbf{y}_i^k \leftarrow \mathbf{x}_i^k$ 
23   if Equation (16) then
24      $\mathbf{z}^k \leftarrow \arg \min_{\mathbf{y}_i^k} \bar{f}|_{\mathbf{y}_i^k}$ 
25      $k^{\text{stall}} \leftarrow 0$ 
26   else
27      $k^{\text{stall}} \leftarrow k^{\text{stall}} + 1$ 
28    $w^{k+1} \leftarrow$  Apply Equation (17)
```

5 Empirical assessment

This section provides the empirical assessment of the proposed approach via two different applications. The first, given in Section 5.3, concerns a simplified setting that is instrumental to show that RATS described in Section 4 can find a solution in the optimal solution set corresponding to the lowest objective function value. Indeed, although the initial portfolio is made of hundreds of instruments of different kinds, the cardinality of the solution space is tractable (roughly of the order of 10^8), and it is possible to find the optimal objective function value and the associated optimal solution set via brute force. This first application is also helpful

Table 1: Composition, values and sensitivities of $\langle \mathcal{P}, \mathbf{p} \rangle$, and its constituents. Specifically, we report aggregate values at the type level for the latter. Market data as of September 2018, the 28th.

| Instrument | Number | $v^{\mathcal{P}}$ (EUR) | $\Delta^{\mathcal{P}}$ (EUR) | $\mathcal{V}^{\mathcal{P}}$ (EUR) | $\Gamma^{\mathcal{P}}$ (EUR) |
|------------------|--------|-------------------------|------------------------------|-----------------------------------|------------------------------|
| Stocks | 75 | 13 465 008 | 134 650 | 0 | 0 |
| Futures | 14 | 0 | -232 792 | 0 | 0 |
| European options | 10 | 99 177 | -20 042 | 12 159 | 7520 |
| American options | 28 | 236 664 | 73 529 | 67 391 | 7424 |
| Total | 127 | 13 800 849 | -44 655 | 79 550 | 14 944 |

to point out the main differences between the proposed approach and a Markowitz-like approach.

The second application concerns a more real setting where the initial portfolio is still the same, but the set of instruments for building the EOS is larger, and the cardinality of the solution space is roughly of the order of 10^{110} . In this case, finding the optimal value of the objective function via brute force is not computationally feasible.

5.1 Experimental setting

Throughout the section, we use the diacritics $\tilde{}$ (tilde) when we refer to the quantities involved in the RATPO problem to emphasize that we are in a specific application setting. Below are the specifications for the initial portfolio, for the objective function f , and for the constraints determining the feasible set of EOS, namely $\tilde{\mathcal{E}}$, used in both applications. These specifications are needed to pose the RATPO problem ($\tilde{\text{P1}}$) tackled in our empirical assessment, that is, a particular case of (P1).

Initial portfolio We consider a real trading portfolio $\langle \mathcal{P}, \mathbf{p} \rangle$ including 127 financial instruments in 6 different currencies on 87 underlying equity stocks and indices, as reported in Table 1. The initial portfolio composition, features, and risk measures reflect the trader’s view at t , i.e., as of September 28, 2018. The initial portfolio static UIs are determined by parameters ϕ_i , such as underlying, payoff type, maturity, and strike (see Section 2). We consider five features for the static UIs, namely the value, the P&L, and the sensitivities Delta, Vega, and Gamma. The value at t is marked to market. Conversely, in the case of risk scenarios, for stocks and futures, the value is marked to market, whereas for options, it is marked to model, i.e., computed according to specific pricing models.⁷

Starting from the features of the static UIs and exploiting Equation (9), we compute the initial portfolio value $v^{\mathcal{P}}$, its P&L in the risk scenarios, and the sensitivities $\Delta^{\mathcal{P}}$, $\mathcal{V}^{\mathcal{P}}$, $\Gamma^{\mathcal{P}}$. Table 1 provides $v^{\mathcal{P}}$, $\Delta^{\mathcal{P}}$, $\mathcal{V}^{\mathcal{P}}$, and $\Gamma^{\mathcal{P}}$. Additionally, the P&L distribution is given in Figure 1.

Objective function The objective function for the two applications is the same. It consists of the combination of two portfolio risk measures and one portfolio feature. Let us indicate with $\text{P\&L}^{\mathcal{P}}$ the profit we would make in one day by investing $\langle \mathcal{P}, \mathbf{p} \rangle$ at the risk-free rate corresponding to the rebalancing date. As risk measures of interest for the $\langle \mathcal{T}, \mathbf{t} \rangle$ given in Equation (12), we consider the sample P&L, denoted by $\overline{\text{P\&L}}^{\mathcal{T}}$, and the β -VaR $^{\mathcal{T}}$ with $\beta = 1\%$,

⁷We use the model by Black and Scholes 1973 for European options, and the approximation provided by Barone-Adesi and Whaley 1987 for American options. We remark that our approach only requires the usage of non-sophisticated pricing models to manage plain vanilla UEs. Then, the other features are computed by using Equations (1) to (4). More precisely, the sensitivities Delta and Gamma are based on a 1% multiplicative shock of the underlying asset. The sensitivity Vega is based on a 1% additive shock of the implicit volatility of the underlying. All the features are either observed or computed in their reference currencies and then converted to EUR currency. The number of considered risk scenarios is $s = 250$.

defined in Equations (10) and (11), respectively. In our experiments, we consider the β -VaR T as negative-valued. The considered feature is the transaction cost for implementing $\langle \mathcal{T}, \mathbf{t} \rangle$, defined in Equation (9). Please notice that the transaction cost is only determined by the EOS $\langle \mathcal{H}, \mathbf{h} \rangle$ since $\langle \mathcal{P}, \mathbf{p} \rangle$ is fixed. Accordingly, we denote it by $c^{\mathcal{H}}$. Hence, the objective function reads as

$$\tilde{f}(\mathcal{H}, \mathbf{h}; \mathcal{P}, \mathbf{p}) = \frac{\overline{\text{P\&L}}^T - \text{P\&L}^{\mathcal{P}} - c^{\mathcal{H}}}{\beta\text{-VaR}^T - c^{\mathcal{H}}}. \quad (18)$$

Equation (18) provides a cost-adjusted risk measure of $\langle \mathcal{T}, \mathbf{t} \rangle$. The sign of the cost term can be easily understood by noticing that (i) at the numerator the cost term erodes the excess P&L of $\langle \mathcal{T}, \mathbf{t} \rangle$ w.r.t. $\langle \mathcal{P}, \mathbf{p} \rangle$, and (ii) at the denominator it represents an additional loss to that conveyed by the β -VaR T (which is typically already negative).

Ideally, we would like to maximize the numerator and to vanish the denominator. Since at the denominator we approach zero from the left, the more negative the value of \tilde{f} , the better $\langle \mathcal{T}, \mathbf{t} \rangle$. Hence, in our empirical assessment, we aim at minimizing the objective function in Equation (18).

We remark that the objective function in Equation (18) is a particular case of the general objective in Equation (13), and that our approach is not limited to it.

Constraints We consider Delta, Vega, and Gamma sensitivity constraints. These kinds of constraints are common in day-to-day risk management and trading activities. We remark that the proposed approach is general and not limited to this specific choice for the constraints. The sensitivity constraints are defined according to three portfolio features. Indicate with $\Delta^{\mathcal{P}}$ the monetary value of the delta sensitivity for $\langle \mathcal{P}, \mathbf{p} \rangle$, and the same for the vega and gamma sensitivities, $\mathcal{V}^{\mathcal{P}}$ and $\Gamma^{\mathcal{P}}$, respectively. Analogously, we indicate by $\Delta^{\mathcal{H}}$, $\mathcal{V}^{\mathcal{H}}$, and $\Gamma^{\mathcal{H}}$ the monetary value of the considered sensitivities for $\langle \mathcal{H}, \mathbf{h} \rangle$. Hence, given $\tau^{\Delta}, \tau^{\mathcal{V}}, \tau^{\Gamma} \in \mathbb{R}^+$, the sensitivity constraints read as

$$\begin{aligned} \tilde{\psi}^{\Delta}(\mathcal{H}, \mathbf{h}; \mathcal{P}, \mathbf{p}) &:= |\Delta^{\mathcal{H}}| - \tau^{\Delta} |\Delta^{\mathcal{P}}| \leq 0; \\ \tilde{\psi}^{\mathcal{V}}(\mathcal{H}, \mathbf{h}; \mathcal{P}, \mathbf{p}) &:= |\mathcal{V}^{\mathcal{H}}| - \tau^{\mathcal{V}} |\mathcal{V}^{\mathcal{P}}| \leq 0; \\ \tilde{\psi}^{\Gamma}(\mathcal{H}, \mathbf{h}; \mathcal{P}, \mathbf{p}) &:= |\Gamma^{\mathcal{H}}| - \tau^{\Gamma} |\Gamma^{\mathcal{P}}| \leq 0. \end{aligned} \quad (19)$$

Given the linearity of the sensitivities in the vector of notional amounts as per Equation (9), the constraints in Equation (19) are linear inequality constraints.

Unique eligible instruments We consider a list of $u \in \mathbb{N}$ underlyings, sorted in lexicographical order. Each underlying is either a stock or a stock index. If the underlying is a stock, we consider as UEIs European vanilla options written on the stock and the stock itself. Conversely, we consider European vanilla options and futures written on the stock index to be UEIs. To formally implement Definition 1 in our empirical assessment, we consider the following parameters:

- $\nu \in [u]$ the position of the underlying within the list of underlyings;
- $\omega \in \{c, p, q, s\}$ the type of the UEI, i.e., “c” for call, “p” for put, “q” for futures, “s” for stock;
- $K \in \{0.10, 0.25, 0.50\}$ the strike expressed as Δ -percentage;
- $T \in \mathcal{D}^{T_1} \cup \dots \cup \mathcal{D}^{T_u}$ the time-to-maturity in days, where \mathcal{D}^{T_ℓ} is the domain corresponding to the underlying at the position $\nu = \ell$ within the list of underlyings.

Please refer to Table 3 in Appendix B for further details regarding the parameters associated with the UEIs. Additionally, recall that we denote by n the cardinality of $\mathcal{U}^{\mathcal{H}}$, i.e., the number of considered UEIs. At this point, we are ready to implement Definition 1 in our application setting.

Implementation of Definition 1 (Unique eligible instrument, UEI). *A unique eligible instrument $H_j \in \mathcal{U}^{\mathcal{H}}$, $j \in [n]$, is the string obtained by the concatenation of the value of the*

parameters

$$\begin{cases} \nu_j, \text{ and } \omega_j, & \text{for stocks;} \\ \nu_j, \omega_j, K_j, \text{ and } T_j, & \text{for European options and futures.} \end{cases} \quad (20)$$

Eligible optimization strategy Next, starting from Implementation of Definition 1, considering the sensitivity constraints in Equation (19), we can specify Definition 2 in our setting.

Implementation of Definition 2 (Eligible optimization strategy). *Given $\Delta^{\mathcal{P}}, \mathcal{V}^{\mathcal{P}}, \Gamma^{\mathcal{P}}$, an eligible optimization strategy $\langle \mathcal{H}, \mathbf{h} \rangle$ is a set $\mathcal{H} \subset \mathcal{U}^{\mathcal{H}}$ of $m \leq n$ UEIs, weighted by the corresponding notional amounts $\mathbf{h} = [h_1, \dots, h_m]^{\top}$, satisfying the sensitivity constraints in Equation (19).*

As mentioned in Section 4, thanks to our parameterization we can focus on those EOS having a precise structure on both the set of selected UEIs \mathcal{H} and corresponding notional amounts in \mathbf{h} . This structure is meant to reflect the prior knowledge of traders and risk managers. Recall that u is the number of underlyings and consider the UEIs sorted in lexicographical order. As an example, concerning the structure of \mathcal{H} , in our applications, we require that the EOS contains at most n^i UEIs for each underlying, thus implying a cardinality upper-bound $|\mathcal{H}| \leq m = n^i u$ for the strategy (see Section 4). Specifically, in our experiments, we consider the case where $n^i = 3$. Additionally, if the underlying is a stock we require that \mathcal{H} contains (at most) two vanilla options written on the underlying and the stock itself; if a stock index, (at most) two vanilla options and a futures written on the underlying. This is useful in showing how it is possible to control the size of the EOS—which is important from the operational viewpoint—and how to favor balanced solutions.

Starting from Equation (14), we know that the particle position \mathbf{x} is a $2m$ -dimensional integer vector. The first m entries correspond to the indices of the UEIs, and the second to their notional amounts. Hence, to impose the above structure onto \mathcal{H} , we partition the first m entries of \mathbf{x} into triplets, each corresponding to the $n^i = 3$ UEIs for a specific underlying:

$$\underbrace{x_{1,1}, x_{1,2}, x_{1,3}}_{1^{\text{st}} \text{ underlying}}, \dots, \underbrace{x_{\ell,1}, x_{\ell,2}, x_{\ell,3}}_{\ell^{\text{th}} \text{ underlying}}, \dots, \underbrace{x_{u,1}, x_{u,2}, x_{u,3}}_{u^{\text{th}} \text{ underlying}}. \quad (21)$$

Hereinafter, to enhance readability and with a slight abuse of notation, we use a double indexing: the first on triplets, the second on the elements of a triplet. Looking at Equation (21), we have that that the ℓ -th triplet corresponds to those UEIs $H_j \in \mathcal{U}^{\mathcal{H}}$, $j \in [n]$, having $\nu_j = \ell$. Then, within each triplet, we force the first two entries to be European options and the third to be either a stock or a stock index, depending on the nature of the ℓ -th underlying. Again, referring to the ℓ -th triplet within Equation (21), this means that the $x_{\ell,1}$ and $x_{\ell,2}$ correspond to those H_j with $\nu_j = \ell$ and $\omega_j \in \{c, p\}$. Analogously, $x_{\ell,3}$ to those H_j with $\nu_j = \ell$ and $\omega_j = \text{“s”}$ if the ℓ -th underlying is a stock, $\omega_j = \text{“q”}$ if a stock index. Hence, for each entry $x_{\ell,i}$, where $\ell \in [n]$ and $i \in [n^i]$, we specify accordingly the lower and upper bound $[b_{\ell,i}, u_{\ell,i}]$. If $i \in \{1, 2\}$, then $b_{\ell,i}$ is the lower bound of the range of indices corresponding to the UEIs with $\nu_j = \ell$ and $\omega_j = c$, whereas $u_{\ell,i}$ is the upper bound of the range of indices corresponding to the UEIs with $\nu_j = \ell$ and $\omega_j = p$ (notice that “c” precedes “p” and the underlyings are lexicographically sorted). If $i = 3$ and the ℓ -th underlying is a stock, then $b_{\ell,i} = u_{\ell,i}$ is the index of the (only) UEI with $\nu_j = \ell$ and $\omega_j = s$ (see Implementation of Definition 1). Instead, if the ℓ -th underlying is a stock index, then $b_{\ell,i}$ is the lower bound of the range of indices corresponding to the UEIs with $\nu_j = \ell$ and $\omega_j = q$, $u_{\ell,i}$ the upper bound.

Concerning the notional amounts in \mathbf{h} , the partition in Equation (21) entails a partition on the second m entries of \mathbf{x} corresponding to the notional amounts:

$$\underbrace{x_{m+1,1}, x_{m+1,2}, x_{m+1,3}}_{1^{\text{st}} \text{ underlying}}, \dots, \underbrace{x_{m+\ell,1}, x_{m+\ell,2}, x_{m+\ell,3}}_{\ell^{\text{th}} \text{ underlying}}, \dots, \underbrace{x_{m+u,1}, x_{m+u,2}, x_{m+u,3}}_{u^{\text{th}} \text{ underlying}}. \quad (22)$$

In our empirical assessment, we consider minimum and maximum notional amounts for each entry $x_{m+\ell,i}$, where $\ell \in [u]$ and $i \in [n^i]$, denoted by $\ell_{\ell,i}$ and $t_{\ell,i}$, respectively. Table 3 provides the latter values. Furthermore, the ranges $[\ell_{\ell,i}, t_{\ell,i}]$ are discretized according to the procedure detailed in Appendix B. This is instrumental in showing how easy it is to handle cases where there is an operational need to trade batches of shares.

Starting from Implementation of Definition 2, considering the structure for the set of UEs and notional amounts detailed above, we denote by $\tilde{\mathcal{E}}$ the resulting EOS set.

RATPO problem Starting from the objective function in Equation (18), considering Implementation of Definition 2 and $\tilde{\mathcal{E}}$ given as above, we pose the implementation of the general RATPO Problem 1 we aim at solving in the applications in Sections 5.3 and 5.4.

Implementation of Problem 1. *Given an initial portfolio $\langle \mathcal{P}, \mathbf{p} \rangle$, the total portfolio that optimizes the objective function in Equation (18) subject to the sensitivity constraints in Equation (19) is given by $\langle \mathcal{T}^*, \mathbf{t}^* \rangle := \left\langle \mathcal{P} \uplus \mathcal{H}^*, \left[\mathbf{p}^\top, \mathbf{h}^{*\top} \right]^\top \right\rangle$, where*

$$\langle \mathcal{H}^*, \mathbf{h}^* \rangle = \arg \min_{\langle \mathcal{H}, \mathbf{h} \rangle \in \tilde{\mathcal{E}}} \frac{\overline{\text{P\&L}}^\mathcal{T} - \text{P\&L}^\mathcal{P} - c^\mathcal{H}}{\beta\text{-VaR}^\mathcal{T} - c^\mathcal{H}}. \quad (\widetilde{\text{P1}})$$

We denote the set of optimal solutions by $\tilde{\mathcal{E}}^*$.

Unfortunately, $(\widetilde{\text{P1}})$ is nonconvex. First, the fractional objective function contains the $\beta\text{-VaR}^\mathcal{T}$ at the denominator, which is inherently nonconvex (Lwin, Qu, and MacCarthy 2017 and refs. therein). Second, the EOS set $\tilde{\mathcal{E}}$ is nonconvex as well due to the structure we impose on \mathcal{H} (see paragraph ‘‘Eligible optimization strategy’’ above). Indeed, from a canonical optimization perspective, imposing this structure boils down to a group-wise cardinality constraint on the $\ell_0\text{-norm}^8$ of \mathbf{h} , which is nonconvex.

Although we do not exclude the possibility of deriving a convex surrogate of Equation (18) (Wozabal, Hochreiter, and G. C. Pflug 2010 and refs. therein), and approximating with differentiable functions the (group-wise) cardinality constraint as proposed by Malek-Mohammadi et al. 2016, we believe that such an investigation for deriving an alternative (gradient-based) optimization approach is beyond the scope of our empirical assessment, aimed at demonstrating the relevance of the RATPO problem and the general applicability of RATS given in Algorithm 1.

5.2 Comparison with the Markowitz-like approach

Before delving into the case studies, we relate our approach to a possible variation of the Markowitz mean-variance optimization framework, focusing on the challenges to be addressed for solving $(\widetilde{\text{P1}})$ with a Markowitz-like approach.

The M-approach In his seminal work, Markowitz 1952 defines the portfolio selection problem in terms of expected returns and the variance of returns of n^a assets composing an investment universe $\mathcal{U} := \{A_1, \dots, A_{n^a}\}$. Indicate with $\mathbf{y} = [y_1, \dots, y_{n^a}]^\top$, $\mathbf{y} \in \mathbb{R}^{n^a}$, the vector of portfolio weights for the assets in \mathcal{U} . Assume that the portfolio is fully invested, i.e., $\sum_{j \in [n^a]} y_j = 1$. Denote by $\mathbf{z} := [z_1, \dots, z_{n^a}]^\top$, $\mathbf{z} \in \mathbb{R}^{n^a}$, the vector of assets returns. Indicate with $\boldsymbol{\mu} = \mathbb{E}[\mathbf{z}]$, $\boldsymbol{\mu} \in \mathbb{R}^{n^a}$, the assets expected returns, and assume the covariance matrix $\boldsymbol{\Sigma} = \mathbb{E}[(\mathbf{z} - \boldsymbol{\mu})(\mathbf{z} - \boldsymbol{\mu})^\top]$, $\boldsymbol{\Sigma} \in \mathbb{R}^{n^a \times n^a}$, to be positive-definite. Hence, the portfolio expected return and variance read as:

$$(i) \quad \mu(\mathbf{y}) = \boldsymbol{\mu}^\top \mathbf{y}, \quad (ii) \quad \sigma^2(\mathbf{y}) = \mathbf{y}^\top \boldsymbol{\Sigma} \mathbf{y}. \quad (23)$$

⁸The $\ell_0\text{-norm}$ of a vector is a pseudo-norm defined as the number of nonzero elements in the vector.

By indicating with $\gamma \in \mathbb{R}^+$ the investor risk aversion, exploiting (i) and (ii) in Equation (23), the Markowitz portfolio optimization problem reads as the following quadratic programming problem:

$$\begin{aligned} \mathbf{y}^* = \arg \min_{\mathbf{y}} & \frac{\gamma}{2} \sigma^2(\mathbf{y}) - \mu(\mathbf{y}), \\ \text{subject to} & \sum_{j \in [n^a]} y_j = 1. \end{aligned} \tag{P2}$$

Given the positive-definiteness assumption on Σ , (P2) is convex and thus \mathbf{y}^* exists. Over time, several variants of (P2) have been proposed to consider modifications in the objective function, regularizations, and additional constraints (Perrin and Roncalli 2020 and refs. therein). Notably, the works of Puelz 2001; Larsen, Mausser, and Uryasev 2002; Gaivoronski and G. Pflug 2005; Fabozzi, Huang, and Zhou 2010 represent variants considering β -VaR (and thus the P&L distribution) as a measure of risk. Furthermore, Bertsimas and A. W. Lo 1998 consider the optimization of the vector of instrument notionals instead of \mathbf{y} . Hereinafter, we refer to the above variants of (P2) as M-approaches.

Distinguishing features As mentioned in Section 1, a first distinguishing feature of our approach is that we adopt the viewpoint of bank traders and risk managers, who focus on portfolio risk measurement and features at a given point in time t , and look for optimal trades at the same time t . Mathematically, this means that unlike the M-approach, centered on forward-looking expected values of return and risk, in our approach the relevant portfolio risk measures and features are estimated based on historical scenarios of interest, as given in Section 2.

A second distinguishing feature between the proposed approach and the M-approach concerns the parameterization. Specifically, as given in Equation (14), our optimization variables are the positions of the particles, i.e., $2m$ -dimensional integer vectors each entailing an optimization strategy $\langle \mathcal{H}, \mathbf{h} \rangle$, where $m \leq n$ is the desired cardinality of \mathcal{H} . In contrast, in the M-approach, the variable to be optimized would be a vector of notionals in \mathbb{N}^n , where n is the cardinality of the UEI universe $\mathcal{U}^{\mathcal{H}}$. As shown in the paragraph “Eligible optimization strategy” in Section 5.1, our parameterization allows the user to easily specify a (complex) structure for both \mathcal{H} and \mathbf{h} .

A third distinguishing feature concerns the direct applicability to objective functions of the form in Equation (13), i.e., general combinations of portfolio features and risk measures. Indeed, the objective function in (P2) is convex and, although there are variants of (P2) that consider β -VaR (Fabozzi, Huang, and Zhou 2010 and refs. therein), the fractional form of the objective function in Equation (18) is a challenge for the M-approach. In particular, the nonconvexity and potential non-differentiability of the objective function could impair the direct applicability of the M-approach to the RATPO problem. Specifically, it would be necessary to investigate suitable convex and differentiable surrogates to tackle problems as $(\widetilde{\text{P1}})$, as is done, for example, in the successive convex approximation optimization scheme extensively discussed by Scutari and Sun 2018.

Finally, another distinguishing feature concerns direct applicability in the presence of an arbitrarily complex set of constraints to be handled. In fact, although sensitivity constraints in Equation (19) are linear inequality constraints in the notional amounts (see Equation (9)), the group cardinality constraint entailed by the specified structure for \mathcal{H} would result in a constraint on the ℓ_0 -norm of groups of instruments associated with each underlying, where the groups must discriminate the type of instrument (see paragraph “Eligible optimization strategy” in Section 5.1). Looking at the development of an M-approach for solving $(\widetilde{\text{P1}})$, a possible way to enforce such a structure in the solution would be to replace the entailed group cardinality constraint with a convex regularization term within the objective function based on the mixed ℓ_1/ℓ_2 -norm⁹ of the vector of notional amounts. Acting at the level of the groups, the ℓ_2 -norm would promote sparsity in the solution without causing the vanishing of the notional amounts of

⁹Consider $\mathcal{I} = \{\mathcal{I}_1, \dots, \mathcal{I}_u\}$ partition of $[n]$ and a vector $\mathbf{a} \in \mathbb{R}^n$. Denote by $a_{\nu,i}$ the i -th entry within the

Table 2: $\overline{\text{P\&L}}^{\mathcal{G}}$, $\beta\text{-VaR}^{\mathcal{G}}$, trading cost $c^{\mathcal{G}}$, and corresponding objective function value when $\langle \mathcal{G}, \mathbf{g} \rangle$ is (i) $\langle \mathcal{P}, \mathbf{p} \rangle$, (ii) $\langle \mathcal{T}^*, \mathbf{t}^* \rangle$ for the small-sized EOS case computed via brute-force, and (iii) $\langle \widehat{\mathcal{T}}, \widehat{\mathbf{t}} \rangle$ for the large-sized EOS case retrieved by RATS, in the different settings determined by the value of τ^g . Notice that $\langle \mathcal{P}, \mathbf{p} \rangle$ is the same in all case studies and settings. Additionally, since in the small-sized EOS case RATS retrieves a solution within the optimal solution set (cf. Figure 2), we report only $\langle \mathcal{T}^*, \mathbf{t}^* \rangle$ in the table, as it coincides with the estimated one.

| Portfolio $\langle \mathcal{G}, \mathbf{g} \rangle$ | Case Study | τ^g | $\overline{\text{P\&L}}^{\mathcal{G}}$ (EUR) | $\beta\text{-VaR}^{\mathcal{G}}$ (EUR) | $c^{\mathcal{G}}$ (EUR) | $\tilde{f}(\langle \mathcal{G}, \mathbf{g} \rangle)$ |
|---|---------------|----------|--|--|-------------------------|--|
| $\langle \mathcal{P}, \mathbf{p} \rangle$ | All | All | 33 918 | −735 750 | 0 | −0.0455 |
| $\langle \mathcal{T}^*, \mathbf{t}^* \rangle$ | Small- | 0.10 | 31 875 | −590 677 | 905 | −0.0517 |
| | sized | 0.50 | 32 727 | −585 979 | 1035 | −0.0533 |
| | EOS | 1.00 | 32 634 | −582 060 | 1027 | −0.0535 |
| $\langle \widehat{\mathcal{T}}, \widehat{\mathbf{t}} \rangle$ | Large- | 0.10 | 59 674 | −233 573 | 6570 | −0.2194 |
| | sized | 0.50 | 62 150 | −230 546 | 7733 | −0.2267 |
| | EOS | 1.00 | 61 082 | −222 682 | 7955 | −0.2286 |

an entire group of instruments. Acting within groups, the ℓ_1 -norm would result in the zeroing of the notional amounts of some UEIs belonging to each group. However, such a solution would introduce a bias in estimating the notional amounts, and it may not be possible to satisfy exactly the group cardinality imposed through our approach. Conversely, due to our parametrization (see Equation (14)), the proposed approach easily allows a desired composition to be enforced in the solution.

We believe that developing an M-approach to solve $(\widetilde{\text{P1}})$ is an intriguing research question to investigate, as highlighted by the above challenges to be addressed, thus not only interesting from the operational perspective. We, therefore, plan to tackle this research question in the future.

5.3 Small-sized eligible optimization strategy

In this case, we consider a single underlying, the Euro Stoxx 50 Index (.STOXX50E). Given the discussion in the paragraph “Eligible optimization strategy” of Section 5.1, since the underlying is a stock index, \mathcal{H} has to be composed of only two vanilla options and one future written on the specified underlying. Given the domains corresponding to the Euro Stoxx 50 Index features in Table 3, we have $n = 54$ UEIs. Additionally, we set the values of τ^{Δ} , τ^{ν} , and τ^{Γ} equal to τ^g . We investigate three different sensitivity constraint settings, that is, $\tau^g \in \{0.1, 0.5, 1.0\}$. The latter values represent tight, medium, and loose sensitivity constraints.

Since, in this case, the cardinality of the solution space is of the order of 10^8 , we can compute the optimal value for the objective function in Equation (18) via brute force. Appendix D provides the parameters representing one of the solutions in \mathcal{E}^* , for the three settings. Additionally, Table 2 shows the EUR value of the $\overline{\text{P\&L}}^{\mathcal{G}}$, $\beta\text{-VaR}^{\mathcal{G}}$, and trading cost $c^{\mathcal{G}}$ for $\langle \mathcal{P}, \mathbf{p} \rangle$ and for $\langle \mathcal{T}^*, \mathbf{t}^* \rangle$, along with those of the corresponding objective function, in the three settings.

Even though the $\overline{\text{P\&L}}^{\mathcal{G}}$ is slightly lower, we see that the $\beta\text{-VaR}$ of $\langle \mathcal{T}^*, \mathbf{t}^* \rangle$ is consistently lower than that of $\langle \mathcal{P}, \mathbf{p} \rangle$ in all settings. Regarding the cost, it is null in the case of $\langle \mathcal{P}, \mathbf{p} \rangle$ due to

subgroup ν of \mathbf{a} entailed by \mathcal{I} . Then, the mixed ℓ_p/ℓ_q -norm of \mathbf{a} is

$$\|\mathbf{a}\|_{p,q} := \left(\sum_{\nu=1}^u \left(\sum_{i=1}^{|\mathcal{I}_{\nu}|} |a_{\nu,i}|^p \right)^{\frac{q}{p}} \right)^{\frac{1}{q}}.$$

the absence of transactions. In the case of $\langle \mathcal{T}^*, \mathbf{t}^* \rangle$, the cost is contained and similar in the three settings. Accordingly, the objective function evaluated at $\langle \mathcal{T}^*, \mathbf{t}^* \rangle$ is lower as well.

Looking across the settings τ^g , the objective function evaluated at $\langle \mathcal{T}^*, \mathbf{t}^* \rangle$ improves as τ^g increases. This trend is mainly driven by the reduction in the (cost-adjusted) β -VaR g . This result aligns with the fact that the sensitivity constraints loosen as τ^g increases.

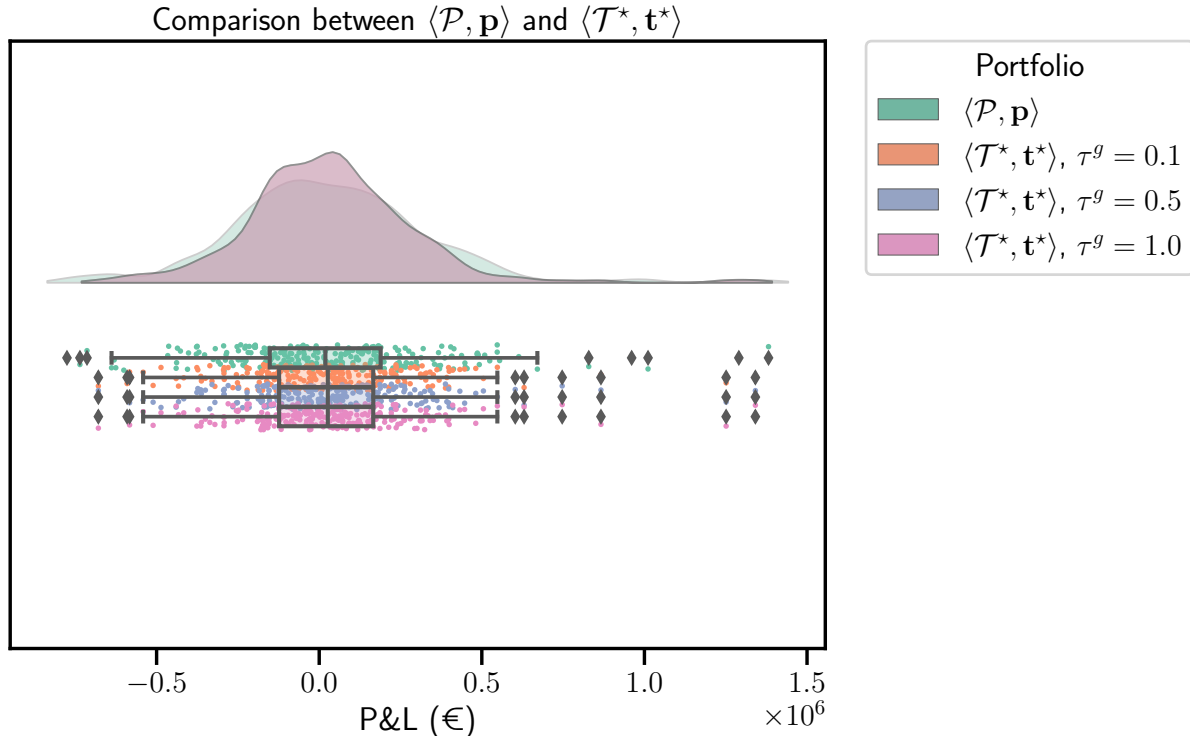


Figure 1: Empirical distribution of the P&L of $\langle \mathcal{P}, \mathbf{p} \rangle$ and $\langle \mathcal{T}^*, \mathbf{t}^* \rangle$, along with the risk scenarios P&L represented as points and overlaid by the corresponding boxplot, for all the investigated settings determined by the value of τ^g .

Additionally, Figure 1 depicts the empirical distribution of the P&L of $\langle \mathcal{P}, \mathbf{p} \rangle$ and $\langle \mathcal{T}^*, \mathbf{t}^* \rangle$, as well as the scenarios P&L overlaid by the corresponding boxplot, for all the investigated settings. Consistently with the provided cost-adjusted β -VaR g reduction, in all the settings $\langle \mathcal{T}^*, \mathbf{t}^* \rangle$ pushes towards zero the left-tail of the distribution of $\langle \mathcal{P}, \mathbf{p} \rangle$. Furthermore, the empirical distributions associated with $\langle \mathcal{T}^*, \mathbf{t}^* \rangle$ are very similar in the three settings.

At this point, to compare the solution retrieved by RATS with the optimal one found via brute force, we solve $(\widetilde{\text{P1}})$ through RATS using $n^p = 1000$ particles, setting $k^{\max} = 500$, and by investigating its behavior when both c^{pers} and c^{soc} take value in the discretized interval $(0., 2.)$, where we move with a step size equal to 0.1. The complete list of the RATS hyper-parameters values is given in Appendix A. We remark that, although the number of particles is large, the time required by RATS to perform the allowed maximum number of iterations for solving $(\widetilde{\text{P1}})$ is only of the order of 10 seconds. This holds also for the second application, see Appendix C for details.

The plots in Figure 2 depict the objective function value corresponding to the solution $\langle \widehat{\mathcal{T}}, \widehat{\mathbf{t}} \rangle$ estimated by RATS, in all the settings and for all the tested hyper-parameters values. Within each plot, we represent with a star \star the case in which our algorithm returns a solution belonging to the optimal solution set $\widetilde{\mathcal{E}}^*$ of the corresponding RATPO problem, i.e., a solution equivalent to that found via brute force.

Our results empirically prove that RATS can retrieve a solution in the optimal solution set in all the settings. In case $\tau^g \in \{0.5, 1.0\}$, the optimal solution is returned for the most pairs of

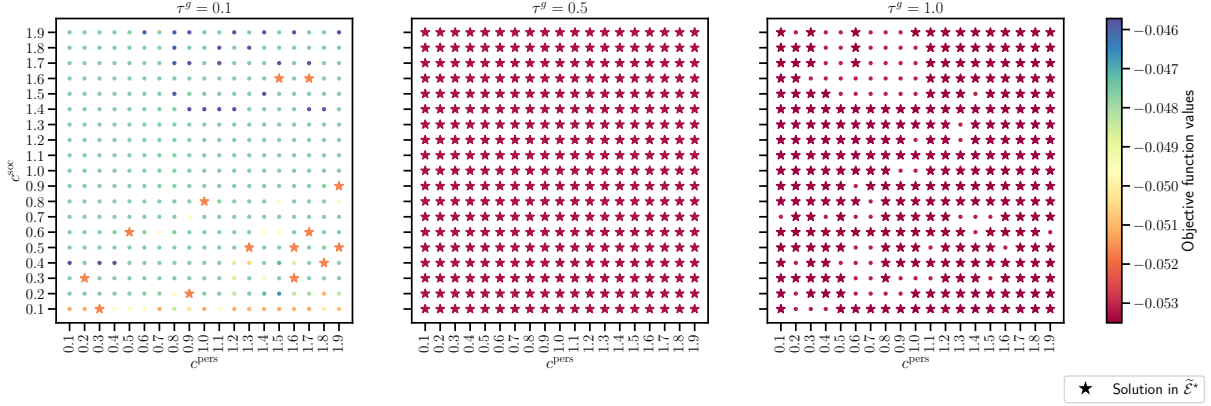


Figure 2: Objective function value corresponding to the solution $\langle \hat{\mathcal{T}}, \hat{\mathbf{t}} \rangle$ estimated by RATS, in all the settings and for all the tested $(c^{\text{pers}}, c^{\text{soc}})$ pairs.

hyper-parameters value $(c^{\text{pers}}, c^{\text{soc}})$, suggesting that RATS is also robust to the hyper-parameters choice when the sensitivity constraints loosen.

Looking at the objective function values related to the color legend in Figure 2, we see that, in case $\tau^g = 0.5$, we have no variation as we always retrieve a solution in the optimal solution set. Regarding the case $\tau^g = 1.0$, most solutions belong to the optimal solution set. We also observe a few nearly optimal solutions, represented as points within the plot, characterized by a dark red color, which is almost indistinguishable from that of the stars. Instead, in the more restrictive case $\tau^g = 0.1$, a consistent color gradient shows up, thus signaling that the fine-tuning of the hyper-parameters value becomes more important when the constraints tighten. Nevertheless, the minima of the objective function in the three settings are close in value.

5.4 Large-sized eligible optimization strategy

In this case, we consider $u = 13$ underlyings. Hence, given the domains in Table 3, we have $n = 620$ UEIs. In this case, the cardinality of the solution space is of the order of 10^{110} . Thus, it is not feasible to compute the optimal objective function value and corresponding $\tilde{\mathcal{E}}^*$ via brute force.

We apply RATS by using the same values for the hyper-parameters as in Section 5.3, provided in Appendix A. Appendix D provides the parameters within $\langle \hat{\mathcal{T}}, \hat{\mathbf{t}} \rangle$ corresponding to the .STOXX50E underlying to enhance the comparison between the two case studies. In addition, Table 2 gives the EUR value of the $\overline{\text{P\&L}}^g$, $\beta\text{-VaR}^g$, and trading cost c^g for $\langle \hat{\mathcal{T}}, \hat{\mathbf{t}} \rangle$, along with those of the corresponding objective function, in the three settings. Overall, we see that RATS consistently improves the $\overline{\text{P\&L}}^g$ while reducing the $\beta\text{-VaR}^g$ of $\langle \mathcal{P}, \mathbf{p} \rangle$. This is also true when we consider the trading cost, which is contained and similar in the three settings. Accordingly, the objective function evaluated at $\langle \hat{\mathcal{T}}, \hat{\mathbf{t}} \rangle$ is consistently lower than that evaluated at $\langle \mathcal{P}, \mathbf{p} \rangle$.

Overall, looking across the settings τ^g , the objective values associated with the retrieved solutions are very close, suggesting that RATS is able to find a suitable EOS also in case of tighter sensitivity constraints. In detail, the objective function evaluated at $\langle \hat{\mathcal{T}}, \hat{\mathbf{t}} \rangle$ slightly improves as τ^g increases. The reduction of the $\beta\text{-VaR}^g$ mainly drives this trend. This result is consistent with that in Section 5.3.

Figure 3 depicts the empirical distribution of the P&L of $\langle \mathcal{P}, \mathbf{p} \rangle$ and $\langle \hat{\mathcal{T}}, \hat{\mathbf{t}} \rangle$, as well as the scenarios P&L overlaid by the corresponding boxplot, for all the investigated settings. Consistently with the provided $\beta\text{-VaR}^g$ reduction, in all the settings $\langle \hat{\mathcal{T}}, \hat{\mathbf{t}} \rangle$ pushes towards zero the left-tail of the distribution of $\langle \mathcal{P}, \mathbf{p} \rangle$. Furthermore, the empirical distributions associated with $\langle \hat{\mathcal{T}}, \hat{\mathbf{t}} \rangle$ are very similar in the three settings. This further confirms that RATS can find a performing EOS in all settings.

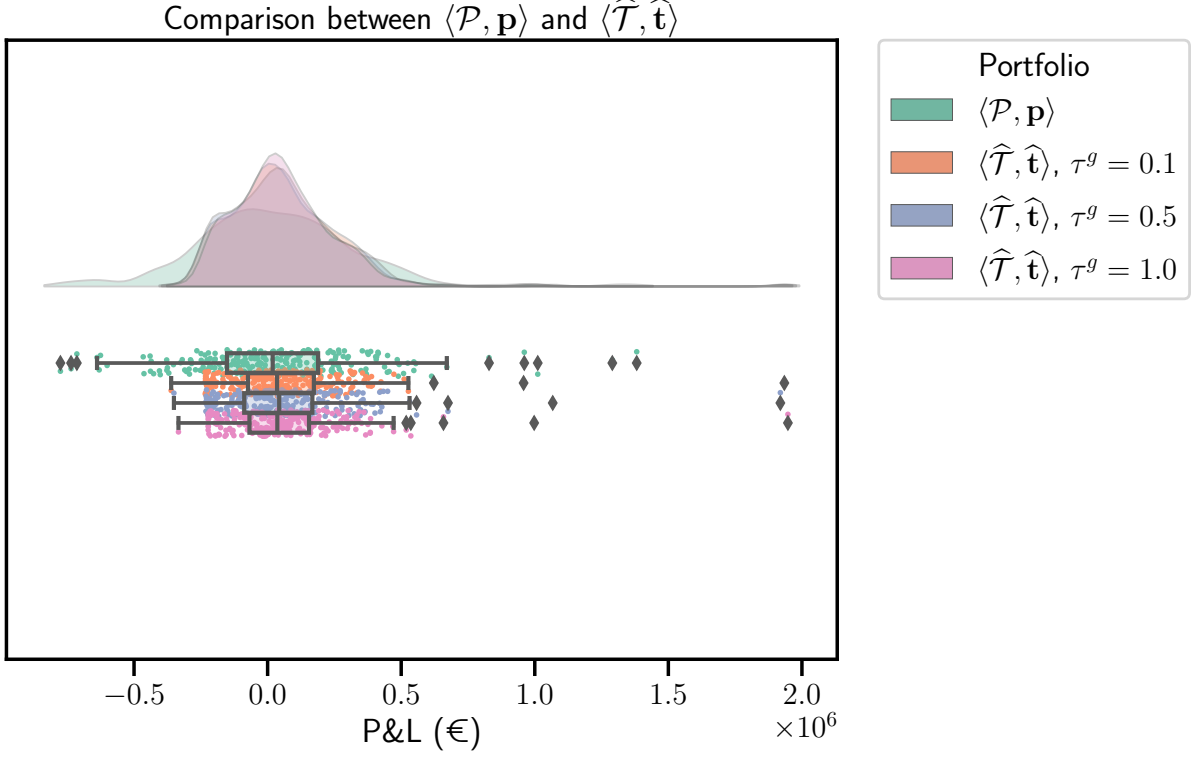


Figure 3: Empirical distribution of the P&L of $\langle \mathcal{P}, \mathbf{p} \rangle$ and $\langle \widehat{\mathcal{T}}, \widehat{\mathbf{t}} \rangle$, along with the risk scenarios P&L represented as points and overlaid by the corresponding boxplot, for all the investigated settings determined by the value of τ^g .

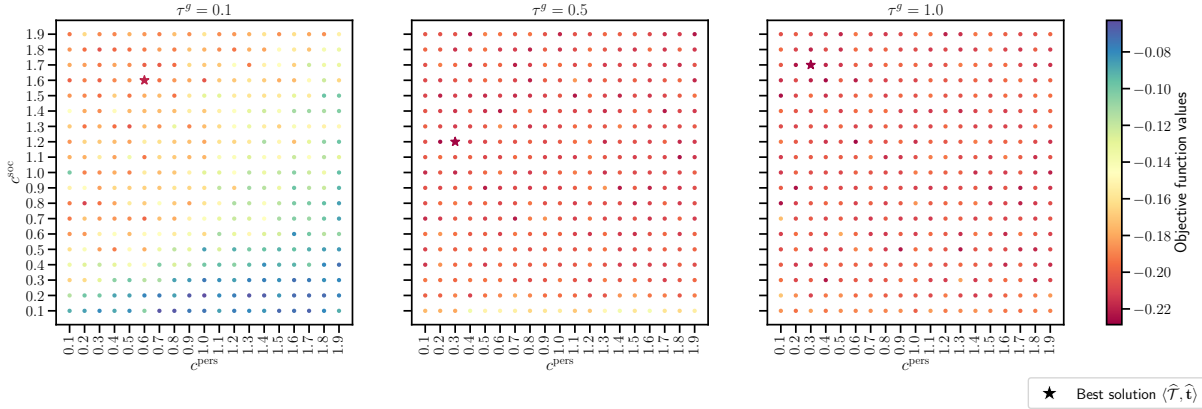


Figure 4: Objective function value corresponding to the solution $\langle \widehat{\mathcal{T}}, \widehat{\mathbf{t}} \rangle$ estimated by RATS, in all the settings and for all the tested $(c^{\text{pers}}, c^{\text{soc}})$ pairs.

Additionally, Figure 4 depicts objective function value corresponding to the solution $\langle \widehat{\mathcal{T}}, \widehat{\mathbf{t}} \rangle$ estimated by RATS, for the three settings and all the considered pairs $(c^{\text{pers}}, c^{\text{soc}})$. In this case, for each setting, we put a star \star in correspondence of the pair of values $(c^{\text{pers}}, c^{\text{soc}})$ that returns the best-estimated solution $\langle \widehat{\mathcal{T}}, \widehat{\mathbf{t}} \rangle$. Looking at Figure 4, in the case of looser sensitivity constraints ($\tau^g \in \{0.5, 1.0\}$), the objective function values corresponding to the retrieved solutions for the different hyper-parameters pairs become closer. This confirms that RATS is robust to the hyper-parameters choice when the sensitivity constraints loosen, as observed in Section 5.3. Additionally, in the case of tighter sensitivity constraints ($\tau^g = 0.1$), the quality of the retrieved solution improves as we move toward the top-left corner of the grid. This suggests that, from

the particle viewpoint, having a stronger tilt toward the global best position at each iteration is beneficial to navigating the more challenging solution space.

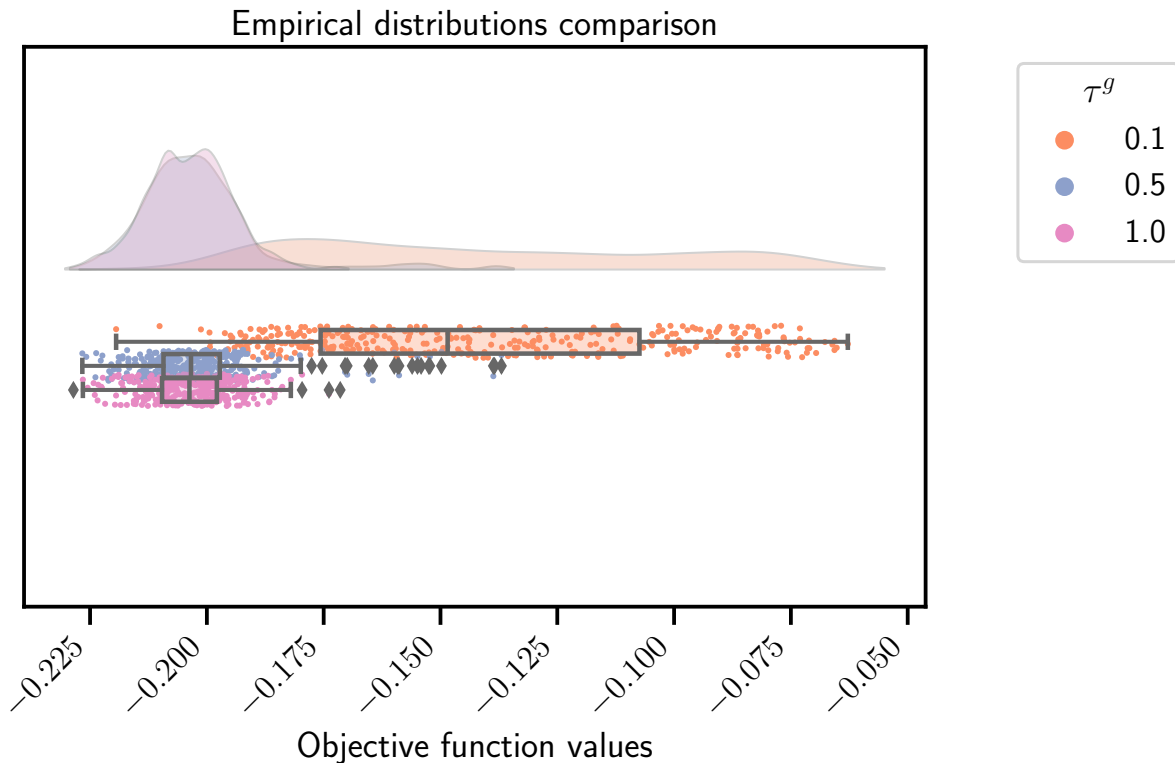


Figure 5: Empirical distributions of the objective function corresponding to the solution $\langle \hat{\mathcal{T}}, \hat{\mathbf{t}} \rangle$ estimated by RATS, in all the settings and for all the tested $(c^{\text{pers}}, c^{\text{soc}})$ pairs.

Finally, Figure 5 shows the empirical distributions of the objective function values in the three settings. Consistently with the discussion above, the distribution spread is lower in case $\tau^g \in \{0.5, 1.0\}$. Nevertheless, the three minima are close in value.

6 Conclusions and perspectives

We proposed and investigated the *risk-aware trading portfolio optimization problem* (RATPO), which takes the point of view of a bank’s traders and risk managers, looking for optimal trades to reduce capital reserves while preserving portfolio value, consistently with the business objectives and limits. The problem solution leverages the basic financial concepts of unique eligible instruments and optimization strategies.

We developed RATS, a versatile computational tool that leverages the parallelizable nature of the optimization problem with respect to the particle dimension. RATS can be adapted to different trading portfolios, objective functions, and constraints. Furthermore, RATS may incorporate the financial insights and business views of traders and risk managers.

We provided a comprehensive numerical evaluation of the proposed approach through two real-world applications on trading portfolios. In the first application, we demonstrated the ability of RATS to identify an optimal solution set, highlighting its advantages over M-approaches.¹⁰ In the second application, we considered 13 underlyings and 620 unique eligible instruments, where the solution space grows to the order of 10^{110} . We demonstrated that RATS was able to scale

¹⁰Recall that we use M-approach to refer to the variants of the quadratic programming problem (P2).

efficiently and handle the complexity of this larger problem, demonstrating its practical utility in large-scale portfolio optimization scenarios.

Our RATPO problem is general with respect to initial portfolios, risk measures and limits, eligible optimization instruments, trading strategies, and optimization algorithms. It can be applied to real portfolios of financial institutions. Strong financial insight is needed both to select the optimization parameters, i.e. the eligible optimization strategies, and to understand the financial soundness of the solutions proposed by RATS. In conclusion, our work bridges the gap between the implementation of effective trading strategies and compliance with stringent regulatory and economic capital requirements, allowing a better alignment of business and risk management objectives.

Future work, as discussed in Section 5.2, could investigate the development of a gradient-based, continuous optimization M-approach to solve $(\widetilde{P1})$. This research direction is relevant from an operational perspective and poses stimulating challenges. For example, a major issue is the non-convexity and potential non-differentiability of the objective function in Equation (18), which may hinder the direct application of these variants to portfolio optimization problems. Addressing this problem would involve the exploration of suitable convex and differentiable surrogates. Moreover, managing the complexities of the feasible set of eligible optimization strategies will be a critical area of our future research. Indeed, the entailed constraints might include non-linear forms, and require methods to promote sparsity in the solutions without biasing the estimation of notional amounts.

References

- Barone-Adesi, Giovanni and Robert E Whaley (1987). “Efficient analytic approximation of American option values”. In: *The Journal of Finance* 42.2, pp. 301–320. DOI: /10.1111/j.1540-6261.1987.tb02569.x.
- Basel Committee on Banking Supervision (June 2011). *Basel III: A global regulatory framework for more resilient banks and banking systems*. URL: <https://www.bis.org/publ/bcbs189.htm>.
- (July 2015). *Corporate governance principles for banks*. URL: <https://www.bis.org/bcbs/publ/d328.htm>.
- (Dec. 2017). *Basel III: finalising post-crisis reforms*. URL: <https://www.bis.org/bcbs/publ/d424.htm>.
- Bertsimas, Dimitris and Andrew W Lo (1998). “Optimal control of execution costs”. In: *The Journal of Financial Markets* 1.1, pp. 1–50. DOI: /10.1016/S1386-4181(97)00012-8.
- Black, Fischer and Myron Scholes (1973). “The pricing of options and corporate liabilities”. In: *Journal of political economy* 81.3, pp. 637–654. DOI: /10.1086/260062.
- Boussaid, Ilhem, Julien Lepagnet, and Patrick Siarry (July 2013). “A survey on optimization metaheuristics”. In: *Information sciences* 237, pp. 82–117. DOI: 10.1016/j.ins.2013.02.041.
- Chang, Tun-Jen, Sang-Chin Yang, and Kuang-Jung Chang (2009). “Portfolio optimization problems in different risk measures using genetic algorithm”. In: *Expert Systems with Applications* 36.7, pp. 10529–10537. DOI: /10.1016/j.eswa.2009.02.062.
- CRD4 (June 2013). “Directive 2013/36/EU of the European Parliament and of the Council of 26 6 2013 on access to the activity of credit institutions and the prudential supervision of credit institutions and investment firms”. In: *Official Journal of the European Union*. URL: <https://eur-lex.europa.eu/eli/dir/2013/36/oj>.
- CRD5 (May 2019). “Directive (EU) 2019/878 of the European Parliament and of the Council of 20 5 2019 amending Directive 2013/36/EU as regards exempted entities, financial holding companies, mixed financial holding companies, remuneration, supervisory measures and powers and capital conservation measures”. In: *Official Journal of the European Union*. URL: <https://eur-lex.europa.eu/eli/dir/2019/878/oj>.

- CRD6 (June 2024). “Directive (EU) 2024/1619 of the European Parliament and of the Council of 31 5 2024 amending Directive 2013/36/EU as regards supervisory powers, sanctions, third-country branches, and environmental, social and governance risks”. In: *Official Journal of the European Union*. URL: <https://eur-lex.europa.eu/eli/dir/2024/1619/oj>.
- CRR1 (June 2013). “Regulation (EU) No 575/2013 of the European Parliament and of the Council of 26 6 2013 on prudential requirements for credit institutions and investment firms and amending Regulation (EU) No 648/2012”. In: *Official Journal of the European Union*. URL: <https://eur-lex.europa.eu/eli/reg/2013/575/oj>.
- CRR2 (June 2019). “Regulation (EU) 2019/876 of the European Parliament and of the Council of 20 5 2019 amending Regulation (EU) No 575/2013 as regards the leverage ratio, the net stable funding ratio, requirements for own funds and eligible liabilities, counterparty credit risk, market risk, exposures to central counterparties, exposures to collective investment undertakings, large exposures, reporting and disclosure requirements, and Regulation (EU) No 648/2012”. In: *Official Journal of the European Union*. URL: <https://eur-lex.europa.eu/eli/reg/2019/876/oj>.
- CRR3 (June 2024). “Regulation (EU) 2024/1623 of the European Parliament and of the Council of 31 5 2024 amending Regulation (EU) No 575/2013 as regards requirements for credit risk, credit valuation adjustment risk, operational risk, market risk and the output floor”. In: *Official Journal of the European Union*. URL: <https://eur-lex.europa.eu/eli/reg/2024/1623/oj>.
- Dallagnol, V.A.F., J. van der Berg, and L. Mous (2009). “Portfolio Management Using Value at Risk: A Comparison between Genetic Algorithms and Particle Swarm Optimization”. In: *International Journal of Intelligent Systems* 24, pp. 766–792. DOI: 10.1002/int.20360.
- Dao, Binh (2014). “Optimal Portfolio with Options in a Framework of Mean-CVaR”. In: *Available at SSRN 2543722*. DOI: /10.2139/ssrn.2543722.
- Das, Akashdeep et al. (2023). “Selection of Appropriate Portfolio Optimization Strategy”. In: *Theoretical and Applied Computational Intelligence* 1.1, pp. 58–81. DOI: 10.31181/taci1120237. URL: <http://www.taci-journal.org/index.php/taci/article/view/7>.
- Deng, Guang-Feng, Woo-Tsong Lin, and Chih-Chung Lo (2012). “Markowitz-based portfolio selection with cardinality constraints using improved particle swarm optimization”. In: *Expert Systems with Applications* 39.4, pp. 4558–4566. DOI: 10.1016/j.eswa.2011.09.129.
- Erekhinsky, Alexei (Oct. 2017). *Searching for a risk target in discrete world*. WBS 13th Fixed Income Conference.
- Ertenlice, Okkes and Can B. Kalayci (2018). “A survey of swarm intelligence for portfolio optimization: Algorithms and applications”. In: *Swarm and Evolutionary Computation* 39, pp. 36–52. ISSN: 2210-6502. DOI: 10.1016/j.swevo.2018.01.009.
- Erwin, Kyle and Andries Engelbrecht (2023a). “Meta-heuristics for portfolio optimization”. In: *Soft Computing* 27.24, pp. 19045–19073. DOI: 10.1007/s00500-023-08177-x.
- (2023b). “Multi-guide set-based particle swarm optimization for multi-objective portfolio optimization”. In: *Algorithms* 16.2, p. 62. DOI: 10.1007/s00500-023-08177-x.
- Fabozzi, Frank J., Dashan Huang, and Guofu Zhou (2010). “Robust portfolios: Contributions from operations research and finance”. In: *Annals of Operations Research* 176, pp. 191–220. DOI: 10.1007/s10479-009-0515-6.
- Faias, José and Pedro Santa-Clara (2011). “Optimal Option Portfolio Strategies”. In: *AFA 2011 Denver Meetings Paper*, 38 pages. DOI: 10.2139/ssrn.1569380.
- Faias, José Afonso and Pedro Santa-Clara (2017). “Optimal Option Portfolio Strategies: Deepening the Puzzle of Index Option Mispricing”. In: *Journal of Financial and Quantitative Analysis* 52.1, pp. 277–303. DOI: 10.1017/S0022109016000831.
- Gaivoronski, Alexei and Gerog Pflug (2005). “Value-at-risk in portfolio optimization: properties and computational approach”. In: *The Journal of Risk* 7 (2), pp. 1–31. DOI: 10.21314/JOR.2005.106.

- Gilli, Manfred, Evis Kellezi, and Hilda Hysi (2006). “A data-driven optimization heuristic for downside risk minimization”. In: *The Journal of Risk* 8 (3), pp. 1–18. DOI: 10.21314/JOR.2006.129.
- Green, Andrew (Nov. 2015). *XVA: Credit, Funding and Capital Valuation Adjustment*. Wiley Finance. John Wiley & Sons.
- Gregory, Jon (Apr. 2020). *The Xva Challenge: Counterparty Risk, Funding, Collateral, Capital and Initial Margin*. Wiley Finance. John Wiley & Sons Inc.
- Gunjan, Abhishek and Siddhartha Bhattacharyya (2023). “A brief review of portfolio optimization techniques”. In: *Artificial Intelligence Review* 56.5, pp. 3847–3886. DOI: 10.1007/s10462-022-10273-7.
- Holland, John H. (Apr. 1992). *Adaptation in Natural and Artificial systems*. Complex Adaptive Systems. The MIT Press. ISBN: 9780262581110.
- Jun, Cheng Seng and Farhana Johar (2023). “Portfolio Optimization of Exchange-Traded Funds Listed on the New York Stock Exchange Using Particle Swarm Optimization”. In: *Proceedings of Science And Mathematics*. Vol. 16, pp. 46–57.
- Kennedy, James (2006). “Swarm intelligence”. In: *Handbook of nature-inspired and innovative computing: integrating classical models with emerging technologies*. Springer, pp. 187–219.
- Kennedy, James and Russell Eberhart (1995). “Particle swarm optimization”. In: *Proceedings of ICNN’95 - International Conference on Neural Networks*. Vol. 4. IEEE, pp. 1942–1948. DOI: 10.1109/ICNN.1995.488968.
- Kirkpatrick, S., C. D. Gelatt, and M. P. Vecchi (1983). “Optimization by Simulated Annealing”. In: *Science* 220.4598, pp. 671–680. DOI: 10.1126/science.220.4598.671.
- Kondratyev, Alexei and George Giorgidze (2017). *Evolutionary Algos for Optimizing MVA*.
- Larsen, Nicklas, Helmut Mausser, and Stanislav Uryasev (2002). “Algorithms for Optimization of Value-at-Risk”. In: *Financial Engineering, E-commerce and Supply Chain*. Ed. by Panos M. Pardalos and Vassilis K. Tsitsiringos. Boston, MA: Springer US, pp. 19–46. ISBN: 978-1-4757-5226-7. DOI: 10.1007/978-1-4757-5226-7_2.
- Loke, Zi Xuan et al. (2023). “Portfolio optimization problem: a taxonomic review of solution methodologies”. In: *IEEE Access* 11, pp. 33100–33120. DOI: 10.1109/ACCESS.2023.3263198.
- Lwin, Khin T, Rong Qu, and Bart L MacCarthy (2017). “Mean-VaR portfolio optimization: A nonparametric approach”. In: *European Journal of Operational Research* 260.2, pp. 751–766. DOI: 10.1016/j.ejor.2017.01.005.
- Malek-Mohammadi, Mohammadreza et al. (2016). “Successive concave sparsity approximation for compressed sensing”. In: *IEEE Transactions on Signal Processing* 64.21, pp. 5657–5671. DOI: 10.1109/TSP.2016.2585096.
- Markowitz, Harry (1952). “Portfolio Selection”. In: *The Journal of Finance* 7.1, pp. 77–91. DOI: 10.1111/j.1540-6261.1952.tb01525.x. (Visited on 01/22/2023).
- Perrin, Sarah and Thierry Roncalli (2020). “Machine learning optimization algorithms & portfolio allocation”. In: *Machine Learning for Asset Management: New Developments and Financial Applications*, pp. 261–328. DOI: 10.1002/9781119751182.ch8.
- Puelz, Amy v. (2001). “Value-at-Risk Based Portfolio Optimization”. In: *Stochastic Optimization: Algorithms and Applications*. Ed. by Stanislav Uryasev and Panos M. Pardalos. Boston, MA: Springer US, pp. 279–302. ISBN: 978-1-4757-6594-6. DOI: 10.1007/978-1-4757-6594-6_13. URL: https://doi.org/10.1007/978-1-4757-6594-6_13.
- Rockafellar, R. Tyrrel and Stanislav & Uryasev (Apr. 2000). “Optimization of conditional value-at-risk”. In: *The Journal of Risk* 2 (3), pp. 21–41. DOI: 10.21314/JOR.2000.038.
- Rosenberg, Gili et al. (June 2016). “Solving the Optimal Trading Trajectory Problem Using a Quantum Annealer”. In: *IEEE Journal of Selected Topics in Signal Processing* 10.6, pp. 1053–1060. DOI: 10.1109/JSTSP.2016.2574703.
- Scutari, Gesualdo and Ying Sun (2018). “Parallel and Distributed Successive Convex Approximation Methods for Big-Data Optimization”. In: *Multi-agent Optimization: Cetraro, Italy 2014*.

- Ed. by Francisco Facchinei and Jong-Shi Pang. Cham: Springer International Publishing, pp. 141–308. ISBN: 978-3-319-97142-1. DOI: 10.1007/978-3-319-97142-1_3.
- Shi, Yuhui and Russell Eberhart (1998). “A modified particle swarm optimizer”. In: *1998 IEEE International Conference on Evolutionary Computation Proceedings. IEEE World Congress on Computational Intelligence (Cat. No. 98TH8360)*, pp. 69–73. DOI: 10.1109/ICEC.1998.699146.
- Soleimani, Hamed, Hamid Reza Golmakani, and Mohammad Hossein Salimi (2009). “Markowitz-based portfolio selection with minimum transaction lots, cardinality constraints and regarding sector capitalization using genetic algorithm”. In: *Expert Systems with Applications* 36.3, Part 1, pp. 5058–5063. ISSN: 0957-4174. DOI: 10.1016/j.eswa.2008.06.007.
- Venturelli, Daniele and Alexei Kondratyev (Apr. 2019). “Reverse quantum annealing approach to portfolio optimization problems”. In: *Quantum Machine Intelligence* 1.6, pp. 17–30. DOI: 10.1007/s42484-019-00001-w.
- Wozabal, David, Ronald Hochreiter, and Georg Ch Pflug (2010). “A difference of convex formulation of Value-at-Risk constrained optimization”. In: *Optimization* 59.3, pp. 377–400. DOI: 10.1080/02331931003700731.

Appendix A Hyper-parameters

Here we provide the detailed values of the hyper-parameters for the RATS in Algorithm (1) used in the empirical assessment in Section 5.

- Number of particles $n^p = 1000$;
- Particle personal coefficient

$$c^{\text{pers}} \in \{0.1, 0.2, 0.3, 0.4, 0.5, 0.6, 0.7, 0.8, 0.9, 1.0, 1.1, 1.2, 1.3, 1.4, 1.5, 1.6, 1.7, 1.8, 1.9\};$$

- Particle social coefficient

$$c^{\text{soc}} \in \{0.1, 0.2, 0.3, 0.4, 0.5, 0.6, 0.7, 0.8, 0.9, 1.0, 1.1, 1.2, 1.3, 1.4, 1.5, 1.6, 1.7, 1.8, 1.9\};$$

- Particle maximum velocity $v^{\text{max}} = 1.0$;
- Particle minimum velocity $v^{\text{min}} = -1.0$;
- Particle maximum inertia $w^{\text{max}} = 1.0$;
- Particle minimum inertia $w^{\text{min}} = 1.0$;
- Significance threshold $\tau^f = 10^{-4}$;
- Concentration threshold for the particle population $\tau^p = 0.75$.
- Maximum number of iteration $k^{\text{max}} = 500$;
- Maximum number of of stall iteration $k^{\text{max stall}} = 100$.

Appendix B Data for UEIs

Table 3 shows the considered underlyings for the empirical assessment in Section 5, as well as the corresponding parameters to determine the UEIs according to Implementation of Definition 1.

The ranges of the notional amounts for the options were selected to cover the Vega sensitivity of the initial portfolio, namely \mathcal{V}^p . The ranges for stocks and futures were selected to cover the Delta sensitivity of the initial portfolio, namely Δ^p . Specifically, $\forall \ell \in [u]$, indicate with Δ_ℓ^c and Δ_ℓ^p the Delta sensitivity of the at-the-money (ATM) call and put options with the highest maturity associated with the ℓ -th underlying. Analogously, $\forall \ell \in [u]$, indicate with \mathcal{V}_ℓ^c the Vega

sensitivity of the ATM call option with the highest maturity associated with the underlying. Hence, define

$$\eta_\ell^a := \frac{\mathcal{V}^{\mathcal{P}}}{|\mathcal{V}_\ell^c|}, \quad \text{and} \quad \eta_\ell^b := \frac{\Delta^{\mathcal{P}}}{\max(|\Delta_\ell^c|, |\Delta_\ell^p|)}. \quad (24)$$

At this point, round both η_ℓ^a and η_ℓ^b to the closest hundred, thousand, and so on, depending on the order of magnitude. Mathematically, given $x \in \mathbb{R}$, the applied rounding reads as

$$\bar{x} = \left\lceil \frac{1}{2} \left\lfloor 2 \frac{x}{10^{\lfloor \log_{10}(x) \rfloor}} \right\rfloor \right\rceil \cdot 10^{\lfloor \log_{10}(x) \rfloor}. \quad (25)$$

For instance, according to Equation (25), for $x = 75$ we have $\bar{x} = 80$; for $x = 740$ we have $\bar{x} = 700$. Hence, $\forall \ell \in [u]$, the ranges of notional amounts are given by

$$[\ell_{\ell,i}, t_{\ell,i}] = \begin{cases} [-\bar{\eta}_\ell^a, \bar{\eta}_\ell^a], & \text{if } i \in \{1, 2\}; \\ [-\bar{\eta}_\ell^b, \bar{\eta}_\ell^b], & \text{if } i = 3. \end{cases} \quad (26)$$

Starting from Equation (26), for each $i \in [n^i]$ and $\ell \in [u]$, the domain of the notional amount $\mathcal{D}^{h_{\ell,i}}$ is given by 21 evenly-spaced integer values (including 0) in $[\ell_{\ell,i}, t_{\ell,i}]$.

Table 3: The table shows (i) the considered underlyings divided by category, i.e., stock and stock index; (ii) the parameters to determine for each underlying ℓ the set of UEs relevant for the EOS, that is, $\omega_{\ell,i}$, $K_{\ell,i}$, $T_{\ell,i}$; and (iii) the ranges of the notional associated with the first two instruments (vanilla options) and the third instrument (stock/futures). Specifically, 21 evenly-spaced values have been selected within the specified range (extremes and zero included).

| Category | Underlying | $\omega_{\ell,i}$ | $K_{\ell,i}$ | $T_{\ell,i}$ | $[\ell_{\ell,i}, t_{\ell,i}], i \in [2]$ | $[\ell_{\ell,i}, t_{\ell,i}], i = 3$ |
|-------------|---------------------|-------------------|------------------|---------------------------------|--|--------------------------------------|
| Stock | $\nu = 1$: AXAF.PA | c, p, s | 0.10, 0.25, 0.50 | 21, 49, 84, 168, 266, 630 | [-760 000, 760 000] | [-340 000, 340 000] |
| | 2 : FB.O | c, p, s | 0.10, 0.25, 0.50 | 21, 49, 112, 168, 266, 476, 630 | [-120 000, 120 000] | [-50 000, 50 000] |
| | 3 : GTO.AS | c, p, s | 0.10, 0.25, 0.50 | 21, 49, 84, 168, 266, 630 | [-310 000, 310 000] | [-160 000, 160 000] |
| | 4 : IBM.N | c, p, s | 0.10, 0.25, 0.50 | 21, 49, 112, 168, 266, 476, 630 | [-130 000, 130 000] | [-60 000, 60 000] |
| | 5 : KO.N | c, p, s | 0.10, 0.25, 0.50 | 21, 49, 112, 168, 266, 476, 630 | [-410 000, 410 000] | [-190 000, 190 000] |
| | 6 : ORCL.N | c, p, s | 0.10, 0.25, 0.50 | 21, 49, 84, 168, 266, 476, 630 | [-370 000, 370 000] | [-140 000, 140 000] |
| | 7 : PG.N | c, p, s | 0.10, 0.25, 0.50 | 21, 49, 112, 168, 266, 476, 630 | [-230 000, 230 000] | [-110 000, 110 000] |
| | 8 : T.N | c, p, s | 0.10, 0.25, 0.50 | 21, 49, 112, 168, 266, 476, 630 | [-570 000, 570 000] | [-280 000, 280 000] |
| Stock Index | 9 : .FTMIB | c, p, q | 0.10, 0.25, 0.50 | 21, 49, 84, 168, 266, 630 | [-800, 800] | [-500, 500] |
| | 10 : .FTSE | c, p, q | 0.10, 0.25, 0.50 | 21, 49, 84, 168, 266, 630 | [-2 000, 2 000] | [-2 000, 2 000] |
| | 11 : .GSPC | c, p, q | 0.10, 0.25, 0.50 | 21, 49, 84, 168, 266, 476, 630 | [-7 000, 7 000] | [-3 000, 3 000] |
| | 12 : .NDX | c, p, q | 0.10, 0.25, 0.50 | 21, 49, 84, 168, 266, 476, 630 | [-3 000, 3 000] | [-1 000, 1 000] |
| | 13 : .STOXX50E | c, p, q | 0.10, 0.25, 0.50 | 21, 49, 84, 168, 266, 630 | [-5 000, 5 000] | [-3 000, 3 000] |

Appendix C Running time

This appendix provides details regarding the total running time required by RATS for solving $(\widetilde{P1})$. Since in the two applications given in Sections 5.3 and 5.4 the iterations run by RATS might vary over different simulations (each determined by a specific pair of values $(c^{\text{pers}}, c^{\text{soc}})$), here we monitor the total running time (measured in seconds) divided by the performed number of iterations. We remark that this is not exactly the time per iteration, as the total running time also includes the cost of the initialization (cf. Algorithm 1).

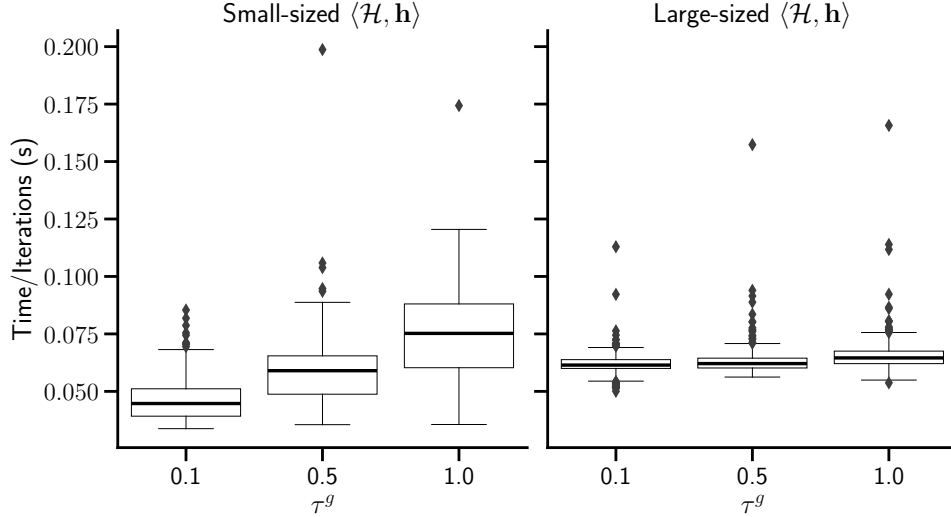


Figure 6: Box plot for the total running time (measured in seconds) divided by the performed number of iterations for (left) the first and (right) second application, and for all the considered values of τ^g . For each application and for each value of τ^g , we create the box plot with the running time and number of iterations associated with the 361 simulations corresponding to the tested pairs $(c^{\text{pers}}, c^{\text{soc}})$.

Figure 6 provides the box plot corresponding to the monitored quantity for (left) the first and (right) second application, and for all the considered values of τ^g . For each application and for each value of τ^g , we create the box plot with the running time and number of iterations associated with the 361 simulations corresponding to the tested pairs $(c^{\text{pers}}, c^{\text{soc}})$. Given the hyper-parameters in Appendix A, from the figure we deduce that the time required by RATS for running k^{max} iterations is roughly of the order of 10 seconds, in both case studies. This empirically proves that performing RATS takes a short time, even when the number of particles is large.

Even though it is beyond the scope of this appendix, from Figure 6 we notice that in the first application, the monitored quantity seems to increase along τ^g , while in the second, it shows no dependence. We hypothesize that one of the causes of this behavior is a side-effect of the usage of just-in-time (JIT) compilation in our code.

When using JIT compilation, there is an initial loading cost due to compiling code at runtime. This cost affects the total execution time, and its impact is larger when the number of iterations that reuse the precompiled code is low.

Figure 7 shows the number of iterations for the tested $(c^{\text{pers}}, c^{\text{soc}})$ for (a) the first and (b) second application. From Figure 7a we see that as τ^g increases, the number of simulations performing a number of iterations lower than k^{max} increases. Hence, the impact of the loading cost increases as well. This explains the (false) dependence on τ^g of the value of the total execution time divided by the number of iterations observed in Figure 7a. Conversely, Figure 7b shows that the number of iterations performed by RATS is roughly the same in all the investigated settings. Accordingly, in this case, we do not observe any dependence in Figure 7b.

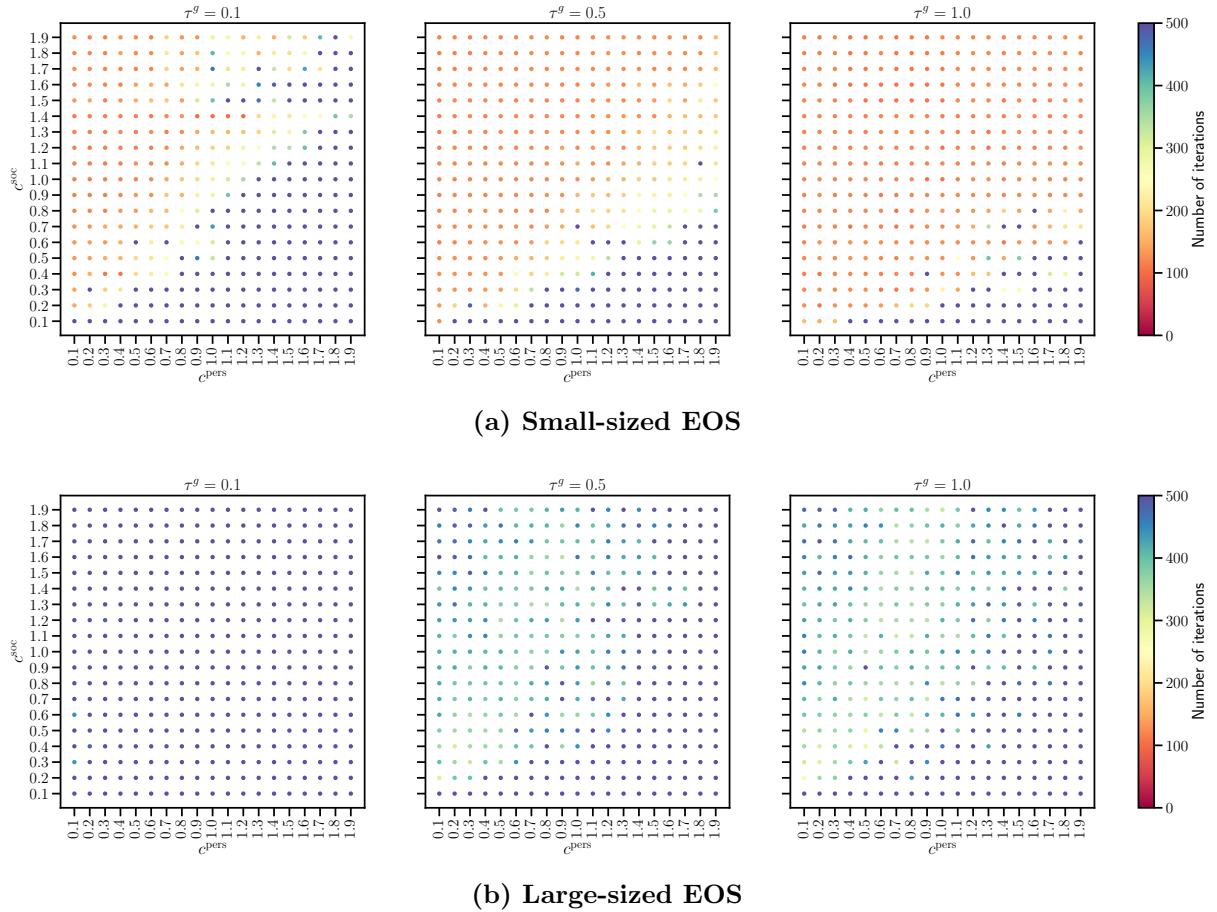
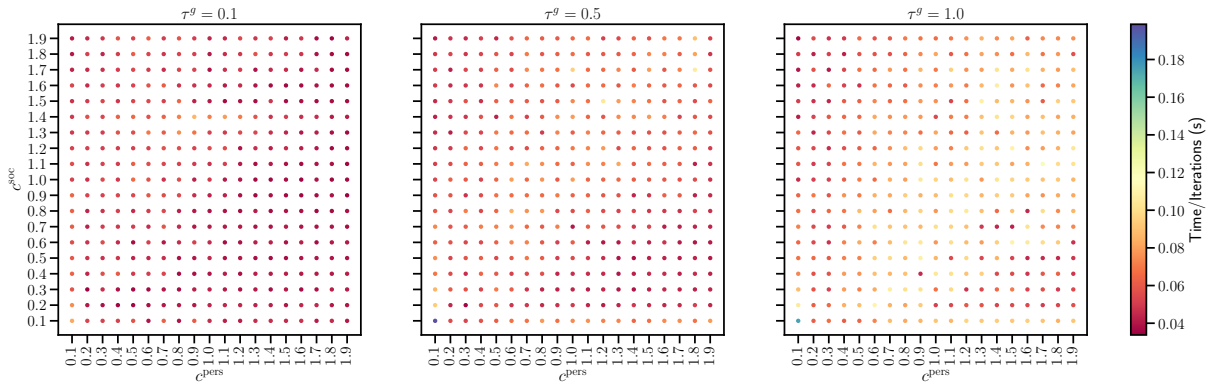


Figure 7: Number of iterations for the tested $(c^{\text{pers}}, c^{\text{soc}})$ for (a) the first and (b) second application.

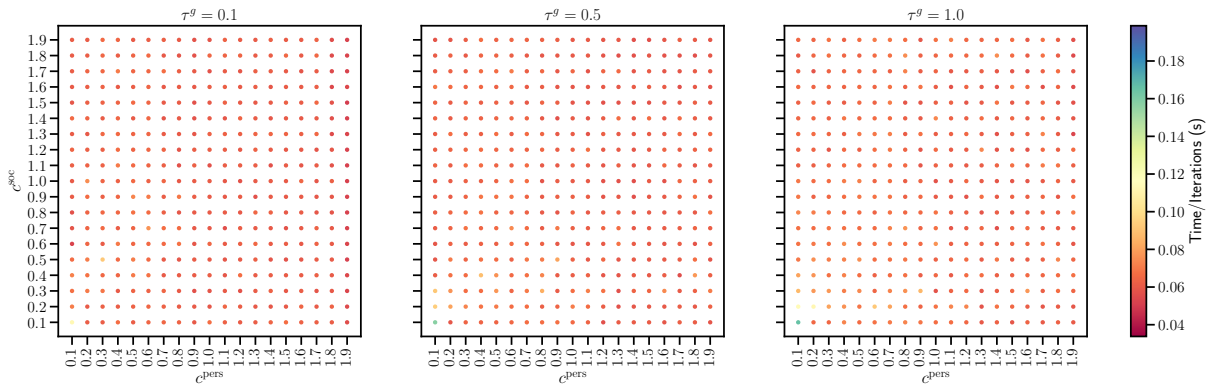
This side-effect is further visualized in Figure 8, which shows that the monitored value tends to be higher for the simulations that are shown to perform a fewer number of iterations for the optimization of the EOS in Figure 7.

Appendix D Estimated parameters for Euro Stoxx 50 Index

Table 4 provides, as an example, the solutions retrieved by RATS for both case studies described in Section 5, for all the investigated settings. As a reminder, in the small-sized EOS case, the solutions estimated by RATS are equivalent to the optimal obtained through brute force. It can be observed that RATS selects varying quantities of call/put options and futures (in the large-sized EOS case, only the .STOXX50E underlying is shown for simplicity), adhering to their respective discrete domains (see Table 3) and the imposed constraints. Notably, in the large-sized EOS case study, the two null notional amount values in the rightmost column indicate instances where RATS identifies simplified trading strategies as more effective, involving only one option rather than two. This behavior is not explicitly favored in our implementation.



(a) Small-sized EOS



(b) Large-sized EOS

Figure 8: Total running time (measured in seconds) divided by the performed number of iterations for (a) the first and (b) second application, and for all the considered values of τ^g .

Table 4: Parameters $\omega_{\ell,i}$, $K_{\ell,i}$, $T_{\ell,i}$, and $h_{\ell,i}$ identifying the selected UEIs and corresponding notionals for the .STOXX50E underlying within the solution retrieved by RATS. We report the parameters' values for all the settings investigated in the empirical assessment provided in Section 5.

| Case Study | Underlying | τ^g | i | $\omega_{\ell,i}$ | $K_{\ell,i}$ | $T_{\ell,i}$ | $h_{\ell,i}$ |
|-----------------|------------|----------|-----|-------------------|--------------|--------------|--------------|
| Small-sized EOS | .STOXX50E | 0.10 | 1 | c | 0.50 | 49 | -3500 |
| | | | 2 | p | 0.25 | 21 | 5000 |
| | | | 3 | q | 0.10 | 21 | 3000 |
| | | 0.50 | 1 | c | 0.50 | 266 | -4500 |
| | | | 2 | p | 0.10 | 49 | 5000 |
| | | | 3 | q | 0.10 | 21 | 3000 |
| | | 1.00 | 1 | c | 0.50 | 266 | -5000 |
| | | | 2 | p | 0.10 | 21 | 5000 |
| | | | 3 | q | 0.10 | 21 | 3000 |
| Large-sized EOS | .STOXX50E | 0.10 | 1 | c | 0.25 | 630 | 0 |
| | | | 2 | c | 0.50 | 168 | -4000 |
| | | | 3 | q | 0.25 | 21 | -600 |
| | | 0.50 | 1 | c | 0.10 | 84 | 0 |
| | | | 2 | c | 0.50 | 630 | -4000 |
| | | | 3 | q | 0.25 | 21 | 600 |
| | | 1.00 | 1 | c | 0.50 | 266 | -3000 |
| | | | 2 | p | 0.10 | 21 | 5000 |
| | | | 3 | q | 0.25 | 21 | 900 |